ANNUAL REVIEWS

Annual Review of Materials Research

Ionic Gating for Tuning Electronic and Magnetic Properties

Yicheng Guan,* Hyeon Han,* Fan Li, Guanmin Li, and Stuart S.P. Parkin

Max Planck Institute of Microstructure Physics, Halle (Salle), Germany; email: stuart.parkin@mpi-halle.mpg.de

Annu. Rev. Mater. Res. 2023. 53:25–51

First published as a Review in Advance on April 17, 2023

The *Annual Review of Materials Research* is online at matsci.annualreviews.org

https://doi.org/10.1146/annurev-matsci-080619-012219

*These authors contributed equally to this article

Keywords

ionic gating, transition metal oxides, magnetic thin films, superconductivity, van der Waals 2D materials, neuromorphic computing

Abstract

The energy-efficient manipulation of the properties of functional materials is of great interest from both a scientific and an applied perspective. The application of electric fields is one of the most widely used methods to induce significant changes in the properties of materials, such as their structural, transport, magnetic, and optical properties. This article presents an overview of recent research on the manipulation of the electronic and magnetic properties of various material systems via electrolyte-based ionic gating. Oxides, magnetic thin-film heterostructures, and van der Waals 2D layers are discussed as exemplary systems. The detailed mechanisms through which ionic gating can induce significant changes in material properties, including their crystal and electronic structure and their electrical, optical, and magnetic properties, are summarized. Current and potential future functional devices enabled by such ionic control mechanisms are also briefly summarized, especially with respect to the emerging field of neuromorphic computing. Finally, a brief outlook and some key challenges are presented.

1. INTRODUCTION

The ever-increasing quantities of digital data that drive modern society require next-generation nanoelectronic memory and computing devices for increased performance, greater functionality, and reduced energy consumption. The basis of many of these devices is the electric-field control of material properties. The archetypical device for such control is the metal–oxide–semiconductor field effect transistor (MOSFET), which is the fundamental element of modern computing architectures (1, 2). In a MOSFET, an electric field is applied between the metal gate and a semiconducting channel across a thin dielectric layer, typically an oxide. Positive and negative gate voltages applied to the metal gate electrostatically induce carriers, either electrons or holes, in the channel in the form of a 2D sheet since the electric field is screened at the dielectric–semiconductor interface. Such a voltage-induced electrostatic doping of carriers into the semiconductor is key to the realization of the transistor function. The MOSFET device that is based on the electric-field control of transport properties in conventional semiconductors has been enormously successful (1, 2), but there are limitations when extending such a structure to other material systems such as transition metal (TM) oxides (3–5), magnetic metallic thin films (6–8), and, most recently, van der Waals (vdW) 2D materials (9, 10). One primary obstacle is the carrier density that is needed for phase transitions in various materials. As an example, TM oxides require much higher induced carrier densities than do conventional semiconductors, resulting in much larger gate voltages that may exceed the breakdown electric-field strength of traditional dielectric layers. Another obstacle comes from the strong surface-screening effects that are the result of the high carrier densities, which limit the penetration length of the electric-field effect to just 1 nm or even a single unit cell (1, 2). These obstacles make the traditional MOSFET structure incompatible with current research goals and make it necessary to find methods that can induce large carrier densities in thin-film materials under modest gate voltages.

The above obstacles can be largely overcome by replacing the traditional dielectric material used in MOSFETs with an electrolyte. The electrolyte is an electrically insulating solid or liquid ionic medium that contains an equal number of positive and negative ions with high mobilities. A typical three-terminal ionic gating device, as shown in **Figure 1*a***, can be realized via gating of the electrolyte (11–14). When a positive gate voltage is applied (**Figure 1*b***), anions in the electrolyte move to the interface between the electrolyte and the gate electrode to compensate for the charge introduced at the gate electrode. Cations, however, migrate and accumulate at the interface between the electrolyte and the target material. To compensate for the charge formed in this way at the electrolyte–target material interface, negative charge accumulates within the target material. The two charged layers of opposite polarity at the interface between the electrolyte and target material lead to the formation of an electric double layer (EDL). As the thickness of the EDL is typically just ~1 nm, the EDL can be considered a nanogap capacitor and thereby has a high specific capacitance and a large electric field. Thus, even a modest gate voltage of just a few volts can lead to very high electric fields of ~10–100 MV/cm, which is significant considering that a conventional MOSFET using a SiO_2 dielectric layer shows an electric-field breakdown limit of ~5–10 MV/cm (11–14). Such high electric fields induced by the thin EDL also allow for relatively low-voltage operation of ionic gating devices.

In addition to the electrostatic effect, the ionic gating approach has recently been found to also lead to an electrochemical effect by which some ions can intercalate or migrate into or out of the target material. This, in turn, changes the composition and properties of the target material (11–27). In fact, ion intercalation from the electrolyte into the solid material was proposed earlier in a two-step intercalation model (28, 29) consisting of the adsorption of ions at the surface of the solid material and the subsequent intercalation of these ions into the solid lattice. The

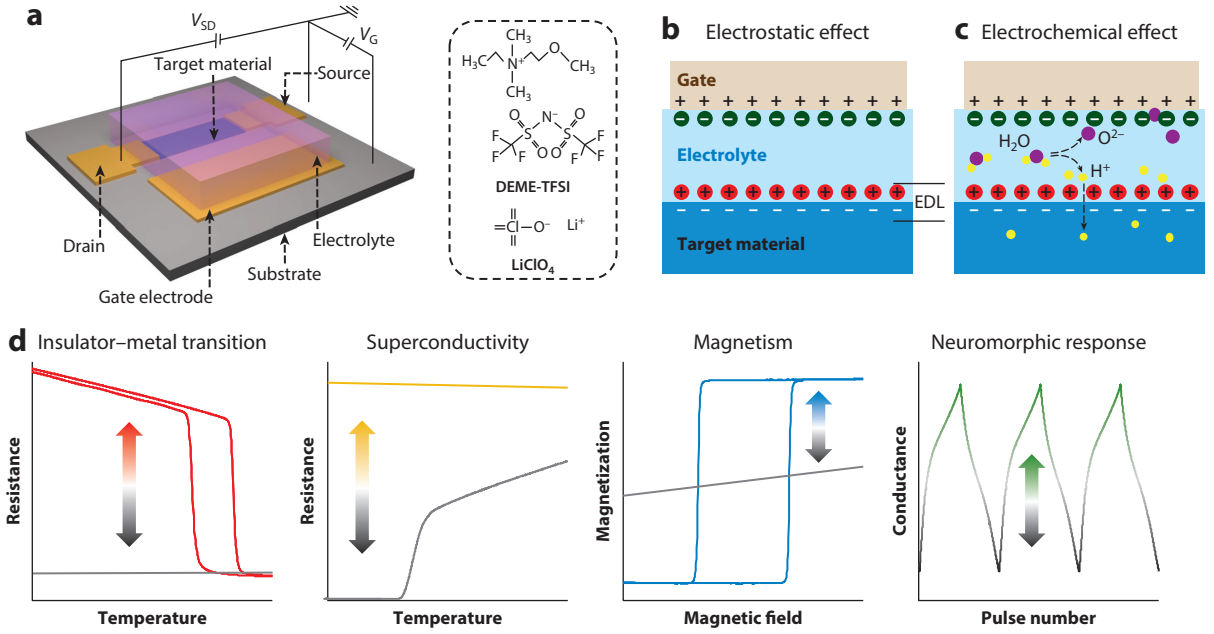

Figure 1

Experimental setup, mechanisms, and physical property tuning via ionic gating. (*a*) Schematic experimental setup of a three-terminal ionic gating device. The inset illustrates two example electrolytes, the ionic liquid DEME-TFSI and the polymer electrolyte containing $LiClO_4$. (*b*,*c*) Schematic illustrations of resulting (*b*) electrostatic and (*c*) electrochemical effects. (*d*) Various physical property changes including an insulator–metal transition, emergent superconductivity, tunable magnetism, and neuromorphic responses induced or controlled via ionic gating. Abbreviations: DEME-TFSI, diethyl methyl(2-methoxyethyl)ammonium bis(trifluoromethyl sulfonyl)imide; EDL, electric double layer; G, gate; $LiClO_4$, lithium perchlorate; SD, source drain.

driving force of such ionic diffusion is the formation of the electric potential gradient across the solid–electrolyte boundary. In particular, conventional ionic liquids absorb water (H_2O) from the environment, thereby leading to the possibility of hydrogen ion (H^+) or oxygen ion (O^{2-}) migration into the target material via ionic liquid gating (30) (**Figure 1*c***). Note that the electrostatic and electrochemical effects are greatly influenced by the nature of the electrolyte and the specific properties of the target material.

The first significant report of an electrochemical effect via electrolyte gating was on thin films of insulating VO_2, where ionic liquid gating was shown to lead to the formation and migration of a comparatively small number of oxygen vacancies (18), which engendered the formation of a metallic state even at very low temperatures. This first report was initially quite controversial because of competing studies that claimed similar effects were electrostatic in origin. However, numerous groups have now confirmed the electrochemical nature of the ionic liquid gate–induced electronic phase transition reported in Reference 18. Indeed, this effect has become widely used and has been applied to a variety of material systems, ranging from TM oxides to metallic thin films and, most recently, 2D vdW materials. Though electrostatic processes can be faster than electrochemical processes, the latter can lead to novel electronic and structural phase transitions along with extensive physical property changes (**Figure 1*d***) that are not possible via conventional electrostatic gating effects. Recent studies have revealed the room-temperature, nonvolatile, and reversible manipulation of physical properties by electrochemical manipulation in diverse material systems (8, 30–34). In addition, electrochemical processes can be used to emulate artificial synapses

with tunable plasticity, which is an important building block for neuromorphic computing (35–40) and for applications where speed is of lesser importance. Thus, the electrochemical approach has significant potential for applications in nanoelectronic devices with ultralow energy consumption, which are the cornerstone of next-generation computing architectures (15–27, 30–33, 35–42).

In this review, we provide an overview of recent research using ionic gating, highlighting the latest advances in the manipulation and control of numerous physical properties in various material systems. Present and potential future functional devices are examined, especially devices relevant for neuromorphic computing. Future perspectives, underlying challenges, and possible solutions are discussed. The TM oxides, magnetic metallic thin films, and vdW 2D materials are the foci of this review as they exhibit rich physics and are being widely investigated as potential platforms for next-generation nanoelectronic devices.

2. ELECTROLYTES FOR IONIC GATING

In recent studies, various types of electrolytes have been used for the manipulation of material properties, including but not limited to inorganic solid electrolytes, polymer electrolytes, ionic liquids, and ion gels. The migrating ions vary from protons and alkali metal ions (cations) to oxygen and hydroxyl ions (anions) (15–27, 41, 42).

Inorganic solid electrolytes, including porous SiO_2 (43), Al_2O_3 (44), HfO_2 (45, 46), and GdO_x (47, 48), are widely used since they offer good chemical and thermal stability with reasonably high ionic conductivities. The most common migrating ions are oxygen ions (O^{2-}) and protons (H^+).

Polymer electrolytes are composed of polymer solvents and diverse ions, among which the alkali metal ions are widely used. A representative polymer electrolyte is formed from a mixture of lithium perchlorate ($LiClO_4$) and polyethylene oxide such that Li^+ and ClO_4^- ions can readily migrate within the polymer matrix. Polymer electrolytes have been used to gate various materials systems ranging from 2D vdW materials to organic single crystals and films (34, 49–51).

Ionic liquids are molten salts composed solely of ions, the melting point of which is typically below room temperature. Compared with the solid electrolytes mentioned above, ionic liquids exhibit higher ionic mobilities and diffusivities due to their weaker interionic interactions, which in turn give rise to faster operation of the devices (11–14). An EDL transistor using an ionic liquid of 1-ethyl-3-methylimidazolium bis(trifluoromethyl sulfonyl)imide (EMIM-TFSI) was first demonstrated in 2007 (52). Later, the ionic liquid diethyl methyl(2-methoxyethyl)ammonium bis(trifluoromethyl sulfonyl)imide (DEME-TFSI) became widely used due to its wider electrochemical stability window and larger interfacial capacitance. Such an ionic liquid gating approach, as compared with solid electrolytes prepared by traditional film deposition methods, can be extended to many different kinds of material systems since the gating effect is nearly independent of interface conditions. An important property of conventional ionic liquids such as EMIM-TFSI and DEME-TFSI is that they contain trace amounts of H_2O, typically more than 100 ppm by mass even after annealing in vacuum (30). This can lead to the introduction of H^+ or O^{2-} into the gated target material. Alternatively, alkali metal ions can be introduced in the ionic liquid. For example, Li^+ ion–doped ionic liquids can lead to faster gate-induced responses (53). In particular, by replacing the conventional Au gate electrode with Li-containing gate electrodes, the Li^+ ions in the electrolyte can be replenished from the Li-containing gate electrode when the Li^+ ions migrate into the target material (53).

Ion gels are made by gelation of a polymer network in an ionic liquid. Therefore, ionic gels can have solid-like stabilities but perform similarly to ionic liquids (11–14). A typical ionic gel electrolyte is formed from a mixture of the ionic liquid 1-butyl-3-methylimidazolium hexafluorophosphate and a triblock copolymer [poly(styrene-block-ethylene oxide-block-styrene)] (54). This electrolyte provided both a large specific capacitance ($>10\ \mu F/cm^2$) and greatly improved

polarization response times (~1 ms) when used as the gate electrolyte in a polymer semiconductor [poly(3-hexylthiophene)] thin-film transistor.

3. IONIC GATE TUNING OF PHYSICAL PROPERTIES OF TRANSITION METAL OXIDES

The use of ionic gating has given rise to a large amount of interesting research concerning the manipulation of various properties of TM oxides. The complex phase diagrams of these materials as a function of oxygen content have made the electric-field control of their electronic phase transitions, including metal to insulator, insulator to metal, or even superconductivity, as well as the manipulation of their magnetic properties (3–5), a very exciting possibility (**Figure 2**). Some examples to date include the following: the ionic gate–controlled phase transition of single crystalline

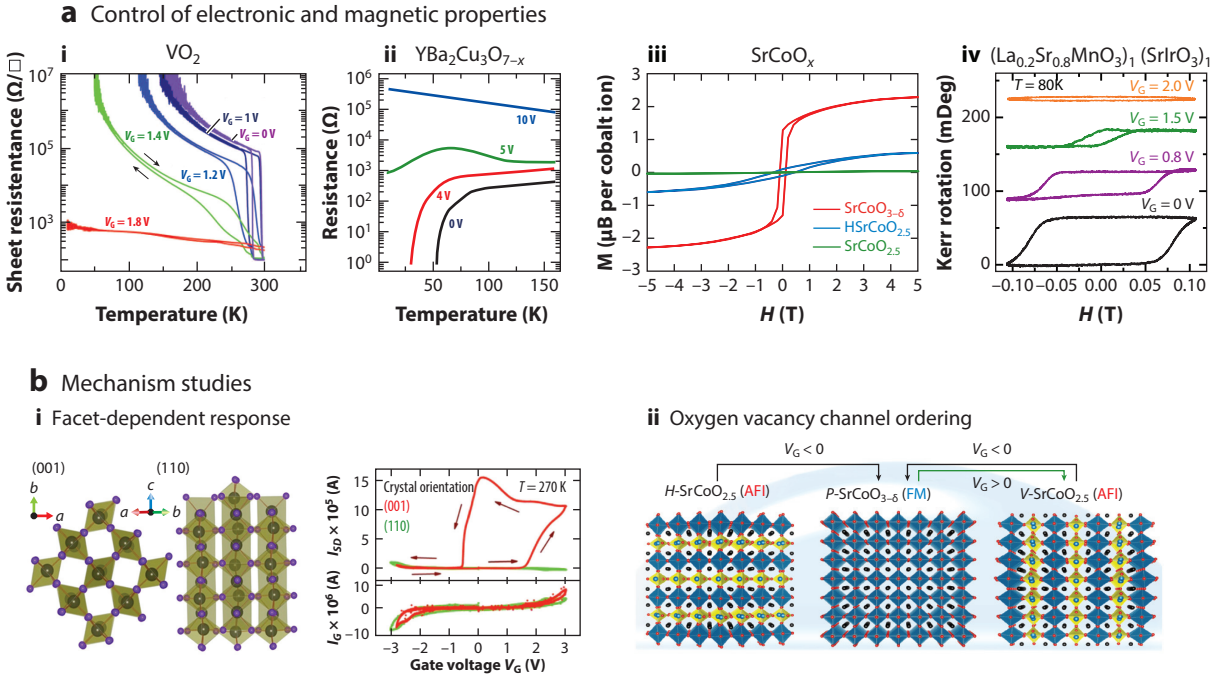

Figure 2

Control of electronic and magnetic properties of transition metal oxides via ionic gating. (*a*, *i*) Temperature dependence of the sheet resistance at various gate voltages of VO_2 films via ionic liquid gating, showing control of the insulator–metal transition. Subpanel adapted with permission from Reference 18; copyright 2018 AAAS. (*a*, *ii*) Temperature-dependent resistance of $YBa_2Cu_3O_{7-x}$ films at several gate voltages, revealing superconductor–metal–insulator transitions of 0 V (*black*), 4 V (*red*), 5 V (*green*), and 10 V (*blue*). Subpanel adapted with permission from Reference 24; copyright 2017 National Academy of Sciences. (*a*, *iii*) In-plane magnetic hysteresis loops of tri-state $SrCoO_x$ (SCO) phases via H^+/O^{2-} ion control. Subpanel adapted with permission from Reference 30; copyright 2017 Springer Nature. (*a*, *iv*) Magnetic hysteresis loops of a superlattice under ionic liquid gating via the in situ magneto-optic Kerr effect, showing voltage control of magnetic properties. Subpanel adapted with permission from Reference 59; copyright 2020 Springer Nature. (*b*, *i*, *left*) Structure of the monoclinic phase of VO_2 along the <001> and <110> axes. (*b*, *i*, *right*) The source-drain (*top*) and gate (*bottom*) current versus the gate voltage V_G of VO_2 thin-film devices for different crystal orientations. Panel adapted with permission from Reference 60; copyright 2015 National Academy of Sciences. (*b*, *ii*) Control of oxygen vacancy channel ordering in $SrCoO_x$ via ionic liquid gating. The antiferromagnetic insulator (AFI) *H*-SCO transforms to ferromagnetic metal (FM) *P*-SCO at a negative gate voltage. A positive gate voltage transforms FM *P*-SCO to AFI *V*-SCO, which can then be reversibly transformed back to *P*-SCO by a negative gate voltage. Panel adapted with permission from Reference 32; copyright 2022 American Chemical Society.

films of $SrTiO_{3-x}$ from an insulating state to a metallic one and, finally, a superconducting state (19, 55); the discovery of superconductivity in $KTaO_3$ crystals via ionic liquid gating (56); the manipulation of high-temperature superconductivity in the family of cuprates such as $YBa_2Cu_3O_{7-x}$ (24) and $La_{2-x}Sr_xCuO_4$ (57); and the modulation of the Curie temperature of $La_{1-x}Sr_xCoO_{3-\delta}$ films over a wide range of temperatures (22, 23). Of special interest is recent progress in ionic gating manipulation of O^{2-} and H^+ ions, the ordering of oxygen vacancies, and crystal facet–dependent responses (30–33, 55–58).

3.1. Electronic Properties of Transition Metal Oxides

One of the most significant findings that has had a long-term impact on today's ionic gating research, especially in the solid-state physics community, is the voltage control of the temperature-dependent insulator–metal phase transition in the binary oxide VO_2 (18, 58). VO_2 becomes a correlated Mott insulator below a characteristic phase transition temperature, above which it is a metal. Jeong et al. (18) found that by applying a gate voltage, using an ionic liquid dielectric, to thin films of VO_2 oriented with the rutile *c*-axis out of plane, the insulator–metal transition (IMT) could be completely suppressed, and the material became conducting down to the lowest temperatures tested (<4 K). Moreover, this suppression was maintained even after removal of the gate voltage (**Figure 2*a***). The mechanism for this nonvolatile gate-controlled IMT was shown to be related to the electric field–induced creation of oxygen vacancies, with the consequent migration of oxygen from within the entire volume of the oxide film into the ionic liquid (18), rather than an electrostatic carrier doping mechanism, as claimed by another group (58). That is, the positive gate voltage applied at the gate electrode induces the removal of oxygen ions in VO_2 and thus creates oxygen vacancies along with electron doping into the lattice. The oxygen vacancy–based mechanism was supported by extensive studies that included the induction of nonvolatility of the gate-induced metallic state, the suppression of the gate-induced IMT under an oxygen atmosphere, spectroscopic confirmation of a significant change in the V valence state, and ^{18}O tracer experiments that showed exchange of oxygen between the ionic liquid and the VO_2 film (18). Another important finding in VO_2 films was that the IMT induced via ionic liquid gating is accompanied by a giant lattice expansion that was more than an order-of-magnitude larger than the lattice contraction that accompanies the temperature-driven insulator-to-metal phase transition in VO_2 (61).

The ionic liquid gate–induced electronic changes in VO_2 thin films are strongly crystal-facet dependent and are observed only when the rutile *c*-axis is oriented perpendicular to the film–ionic liquid interface. The rutile structure is composed of VO_6 octahedra that are edge bonded parallel to the *c*-axis but corner bonded perpendicular to this axis. Thus, there are open structural channels oriented along the *c*-axis that support the migration of oxygen ions into or out of the ionic liquid (60, 62) (**Figure 2*e***). It is interesting that such oxygen ion migration can occur over very long distances of more than 1 μm (63) even though the origin of this migration is the electric fields within the narrow EDL. Presumably oxygen chemical gradients thereby created within the VO_2 layer (both vertically and laterally, depending on the gate electrode geometry) drive the oxygen diffusion over such long distances. Efforts have been made to understand the detailed mechanism of the oxygen vacancy migration process, which is critical for designing future functional oxide devices, but the complex interplay between electrostatic and electrochemical effects and the resulting local changes in structure and electronic properties, all of which depend on distance from the gate electrode, make this very difficult.

An electrochemical mechanism based on oxygen vacancy migration through structural channels was subsequently found to account for ionic gate–induced modulations of the properties of diverse TM oxides (17–27, 30–33, 41, 42, 59, 64–70). One very interesting example is the ionic

liquid gate–induced metallization of the cubic perovskite WO_3, which exhibits no temperature-driven IMT. Nonvolatility and enormous increases in conductivity exceeding ~7 orders of magnitude were found and, moreover, were shown to be independent of the crystal orientation of the WO_3 films (62, 71), presumably originating from the open structural channels along all three principal crystallographic directions (62).

Another example is the brownmillerite $SrCoO_{2.5}$, which is an ideal platform for realizing phase transitions based on ion diffusion due to its well-ordered oxygen vacancy network that results in oxygen vacancy channels (OVCs) along specific crystal directions. A real-time observation of oxygen vacancy migration under ionic liquid gating during the phase transition between the perovskite $SrCoO_3$ state and the brownmillerite $SrCoO_{2.5}$ phase has been directly observed at the atomic level using in situ high-resolution transmission electron microscopy (31). Interestingly, the velocity of the phase transition boundary was shown to be highly anisotropic, traveling laterally ~30 times faster than through the thickness of the film. Such high-speed oxygen transport was attributed to a surface fast oxygen transport lane (31). At the same time, Zhang et al. (33) have shown that oxygen vacancy rows are not only natural oxygen diffusion channels but also preferred sites for the induced oxygen vacancies. Through ionic gating manipulations, Han et al. (32) further identified that the orientations of the OVCs can be switched from horizontal to vertical with respect to the surface of the thin films of $SrCoO_{2.5}$ (**Figure 2*f***).

Oxygen vacancy migration within CuO_x chains induced by ionic gating has been demonstrated to account for the voltage-controlled superconductor–insulator transition in cuprates $YBa_2Cu_3O_{7-x}$ (**Figure 2*b***) and $NdBa_2Cu_3O_{7-x}$, as demonstrated by the nonvolatile nature of the effect, the utilization of oxygen barrier interlayers, and chemical composition analysis using X-ray absorption spectra from thin films during the gating process (24, 64). Whether CuO_x chains are present or not appears to greatly influence ionic gating effects on the cuprates. For example, in the $Pr_{2-x}Ce_xCuO_4$ system where no CuO_x chains are present, gating effects are volatile, suggesting an electrostatic mechanism (64), although it is also possible that oxygen vacancies are created and then removed once the gate voltage is removed. This is the case, for example, for thin TiO_2 layers (72). These results are instructive for the creation of nanoscale structures and interfaces and thus the creation of future oxitronic devices. Prototype 3D mesostructures as well as surface modifications have been realized by taking advantage of anisotropic oxygen vacancy migration (31).

In addition to oxygen vacancy migration–based mechanisms, alkali metal ions and proton-based ionic gating have also been widely investigated in several TM oxide systems. A recent study reports the existence of vertically oriented 2D ionic channels in epitaxial *T*-Nb_2O_5 thin films, which allow for the fast migration of Li^+ ions along the vertical channels via gating (53). This system allows for very-low-voltage operation by Li^+ ion chemical potential control and further shows coupled electronic responses between twin *T*-Nb_2O_5 devices. For ionic gate–induced proton migration, hydrogen intercalation into VO_2 films by ionic liquid gating has recently been explored via nuclear magnetic resonance techniques (73). In another study, hydrogenated VO_2 films were found to show multistep phase transitions, that is, insulator–metal–insulator transitions, with increasing hydrogen concentration (74). By employing this behavior, an all-solid-state proton gating device using a porous silica electrolyte was demonstrated (43).

3.2. Magnetism of Transition Metal Oxides

Beyond electronic phase transitions, the ionic gating approach has been widely used to control the magnetic properties of TM oxide systems; examples include $SrCoO_x$, $SrRuO_3$, $NiCo_2O_4$, and $SrFeO_x$ (30, 65–67). The magnetism in TM oxides arises predominantly from double and superexchange coupling between the magnetic moments of the TM ion via the intermediate oxygen ions.

This means that redox-based chemical reactions induced by ionic gating can strongly influence the valence of the TM ions and in turn tune its magnetism. At the same time, changes in oxygen stoichiometry can affect the structure, even subtly, such as through rotations of the oxygen octahedra or tetrahedra that form the basic structure of these oxides. These structural modifications can therefore influence the magnetic interactions. For example, Lu et al. (30) realized a selective dual-ion switch to control a tristate phase transformation in $SrCoO_{2.5}$ (**Figure 2*c***). Ionic liquid gating was used with dual ions of hydrogen and oxygen. The three different phases were the brownmillerite antiferromagnetic insulator $SrCoO_{2.5}$, the perovskite ferromagnetic metal $SrCoO_{3-x}$, and the hydrogenated weakly ferromagnetic insulator $HSrCoO_{2.5}$. By applying a negative gate voltage, oxygen ions in the ionic liquid migrate to the insulating epitaxial $SrCoO_{2.5}$ thin film, thereby transforming it into the metallic perovskite $SrCoO_{3-x}$ state. A positive gate voltage, in contrast, provides for hydrogen ion migration into the $SrCoO_{2.5}$ layer and results in a transformation to $HSrCoO_{2.5}$. Based on this tristate transformation, Lu et al. (30) realized an electric field–controlled switch of both resistance and magnetism. This work encouraged the exploration of the ionic gate control of multistate phase transitions in several other oxide systems.

The ionic gating approach can also be extended to manipulate magnetism in oxide thin-film heterostructures or even superlattices. Song et al. (68) utilized electric field–controlled dual-ion migration in the epitaxial $SrCoO_{2.5}/La_{0.45}Sr_{0.55}MnO_{3-x}$ (SCO/LSMO) bilayer thin-film system for the manipulation of its magnetic anisotropy. Since different crystal structures can be realized by dual-ion gating within the upper brownmillerite $SrCoO_{2.5}$ layer, a deformation of the MnO_6 octahedral structure occurs at the interface with the lower LSMO layer, thereby leading to a modification of the magnetic anisotropy in this LSMO layer. The interlayer exchange coupling in the oxide heterostructure can also be tuned via ionic gating. In the work of Song et al. (69), a simultaneous tuning of the magnetic anisotropy and exchange bias in $La_{0.8}Sr_{0.2}CoO_3/La_{0.67}Sr_{0.33}MnO_3$ (LSCO/LSMO) heterostructures was obtained though dual-ion migration. A repeated switching of the magnetic easy axis of the bottom LSMO layer between in-plane and out-of-plane directions resulted in a corresponding modulation in the interfacial exchange coupling. The interfacial exchange bias in the $SrFeO_{3-x}/La_{0.7}Sr_{0.3}MnO_3$ (SFO/LSMO) heterostructure has also been modulated by an ionic gate-controlled switching of magnetic order between the antiferromagnetic brownmillerite $SrFeO_{2.5}$ and helimagnetic perovskite $SrFeO_{3-x}$ phases (67, 70). Yi et al. (59) obtained a reversible phase transformation with a large 7% lattice change and a significant modulation in the chemical, electronic, magnetic, and optical properties of superlattices comprised of alternating one-unit-cell-thick layers of $SrIrO_3$ and $La_{0.2}Sr_{0.8}MnO_3$, mediated by the reversible transfer of dual ions through an ionic gating approach (**Figure 2*d***). These results show the high potential for voltage-controlled spintronic devices derived from oxide thin heterostructures and superlattices and suggest that further investigations are likely to be highly fruitful.

4. MAGNETO-IONIC RESEARCH ON MAGNETIC METALLIC THIN FILMS

The manipulation of magnetic properties through electric means would allow for novel, potentially energy-efficient, spin-based storage and logic devices. Ever since the observation of a manipulation of the Curie temperature in magnetic semiconductors, although quite modest, through an electric-field gating effect (75), significant efforts have been devoted to the electric-field control of magnetic properties (75–80). Electric fields have been reported to be effective in controlling not only basic magnetic properties, such as magnetic phase transitions, magnetization, and magnetic anisotropy, but also magnetization dynamics (6–8, 75–80). Significant research into increasing the Curie temperature of magnetic semiconductors to above room temperature was

ultimately unsuccessful, and ferromagnetism in oxide materials is relatively rare compared with antiferromagnetism. For these reasons, magnetic metallic thin-film systems, which exhibit room temperature magnetism with high Curie temperatures and perpendicular magnetic anisotropies, are especially attractive for spintronic applications (81–84). In recent years, magneto-ionic effects using electrolyte-based ionic approaches have become of interest as they have the potential for room-temperature, low-voltage, nonvolatile, and reversible manipulation of magnetic properties (8, 77, 80, 85–90). As discussed in Section 2, in such an approach, by contacting a magnetic metallic thin film with a solid or liquid electrolyte, an applied voltage will engender ionic motion of, for example, oxygen ions and protons, which can then give rise to redox-based electrochemical reactions at the surface or within the interior of the magnetic metallic thin film, thereby affecting its magnetic properties predominantly through control of the oxidation level of the ferromagnetic layer, whether in its bulk or at its surfaces or interface (8, 77, 80, 85–90). In the past few years, numerous magnetic metallic thin-film systems have been investigated through this magneto-ionic approach, including elemental films, heterostructures, and alloys. Here we briefly review recent progress in this field with the magnetic order in metallic thin-film systems varying from ferromagnets and synthetic antiferromagnets to ferrimagnets and antiferromagnets.

4.1. Ferromagnetic Thin Metallic Films

In magnetic metallic thin-film systems, such as Co/Pt heterostructures, the magneto-ionic method has proven to be effective in manipulating diverse magnetic properties including saturation magnetization, uniaxial magnetic anisotropy energy, and coercive fields, most of which result from oxygen-ion migration at the interface of the ferromagnetic layer with the ionic gate electrolytes (80, 86). Recent work has also shown that the proximity-induced magnetic moment in heavy metal layers that are in contact with a ferromagnetic layer, which can be very large, can also be tuned using an ionic gating approach (91). In addition to the magnetic properties mentioned above, the magneto-ionic method has also been utilized to control an asymmetric exchange coupling, namely, the vector exchange Dzyaloshinskii–Moriya interaction (DMI) (92–94). The DMI is key to the formation of a wide variety of chiral, noncollinear spin textures, such as Néel domain walls, and a menagerie of skyrmionic spin textures. The motion of such nanoscopic, chiral magnetic textures, driven by electric current, is fundamental to the realization of racetrack memory devices (81–83, 92–94), which are promising candidates for next-generation nonvolatile memory devices with high performance, high stability, and low energy consumption. In racetrack memory devices, digital data are encoded in the presence or absence of magnetic nanotextures. These nanoscopic textures can be formed from non-collinear topological spin textures, namely skyrmions, whether Bloch or Néel, or more complex objects such as anti-skyrmions or elliptical Bloch skyrmions. To date, however, the most interesting and useful objects are chiral magnetic domain walls that are stabilized in perpendicularly magnetized nanowires (the racetracks) formed from engineered magnetic heterostructures in which the chirality is imposed at interfaces between ultrathin magnetic multilayers (e.g., Co/Ni/Co where the individual layers are just a few angstroms thick) and a heavy metal layer such as Pt or W via an interfacial vector exchange DMI. To avoid long range dipole–dipole interactions that result in coupling of the domain walls within or between neighboring racetracks, the net magnetization of the racetrack can be reduced to nearly zero by creating a synthetic antiferromagnetic racetrack in which two nearly identical magnetic multilayers are formed on top of each other and coupled to one another via an ultrathin antiferromagnetic coupling layer (typically from a ruthenium layer about 7 Å thick) such that the magnetizations in the two multilayers are aligned opposite to one another. It has been shown that the chiral domain walls formed in these complex synthetic antiferromagnetic racetracks can be moved to and along

the racetracks very efficiently at speeds exceeding 1 km/s via nanosecond-long current pulses (83, 95), as discussed further in Section 4.2.

Electrostatic gating methods have been used to achieve voltage control of the DMI and, thereby, skyrmion generation in several systems, such as Ta/CoFeB/TaO_x, Pt/Co/CoO_x, and Ta/IrMn/CoFeB/MgO/Al_2O_3 (46, 96, 97), but magneto-ionic approaches have not been explored much. In recent work, Diez et al. (87) showed an irreversible, nonvolatile change of the DMI in Co/Pt thin-film heterostructures via ionic liquid gating that resulted in oxidation of the Co layers. This, in turn, gave rise to a considerable change in domain-wall motion driven by magnetic fields as compared with prior work on electrostatic gating using the solid-state electrolyte HfO_2 (79). Voltage control using ionic gels combined with strain has been used to modulate the DMI and thereby skyrmion bubbles in the Ta/CoFeB system deposited on a flexible substrate (98). Recently, Zhang et al. (99) have successfully controlled skyrmion generation in a perpendicularly magnetized Mn_2CoAl/Pd thin-film system using ionic liquid gating through both nonvolatile and volatile modifications of the magnetic properties. In comparison to voltage control of skyrmion generation by conventional gating across a nonorganic solid-state oxide electrolyte (46, 96), smaller voltages can be used in the ionic liquid gating case (**Figure 3*a***). These early results have shown that magneto-ionic methods are potentially useful for skyrmion-based research and applications.

4.2. Synthetic Antiferromagnetic Thin Metallic Films

In addition to ferromagnetic metallic systems, the magneto-ionic approach has also been applied to synthetic antiferromagnetic (SAF), ferrimagnetic, and antiferromagnetic thin-film systems. In the SAF system, two magnetic sublayers are separated by a metal spacer that couples them antiferromagnetically through an interlayer exchange coupling known as the Ruderman–Kittel–Kasuya–Yosida interaction (101–103). The SAF system is considered an ideal system for next-generation spintronic devices since it allows for fast magnetization dynamics and high tunability (83, 95, 103). Just as with ferromagnetic metallic thin-film systems, ionic liquid gating can modify the degree of oxidation of the upper magnetic sublayer in the SAF structure closest to the EDL and thus can lead to changes in magnetic properties (87–89). Yang et al. (89) reported tuning of the magnetization reversal process and the hysteresis loops in SAF systems formed from both in-plane magnetized Ta/FeCoB/Ru/FeCoB and out-of-plane magnetized Ta/$(PtCo)_2$/Ru/$(PtCo)_2$ via ionic liquid gating. In recent work by Guan et al. (88), a reversible antiferromagnetic-to-ferromagnetic transition of the sublayers in an SAF structure through ionic liquid gating was reported. The authors showed that this was the result of significant oxidation of the upper magnetic layer in an out-of-plane magnetized Pt/CoNiCo/Ru/CoNiCo SAF system. As a result, an ionic liquid gate–induced change in the current-induced domain wall motion is realized with a much larger magnitude compared with the ferromagnetic case (**Figure 3*b***). This is due to reversible changes, either enhancements or diminishments, in the net imbalance between the magnetization of the two magnetic sublayers, which in turn modify the exchange coupling torque (95) exerted on the SAF domain wall. Guan et al. (88) further designed an ionic liquid gate–controlled device, a domain wall switch, based on the transition between an SAF domain wall and a ferromagnetic domain wall, that demonstrates a magnetic-ionic approach for functional logic devices beyond memory devices.

4.3. Ferrimagnetic Thin Metallic Films

Ferrimagnetic systems have attracted much attention in recent years since they combine key benefits of both ferromagnetic and antiferromagnetic systems. A ferrimagnet is typically composed of two distinct magnetic sublattices, in each of which the magnetic moments are ferromagnetically

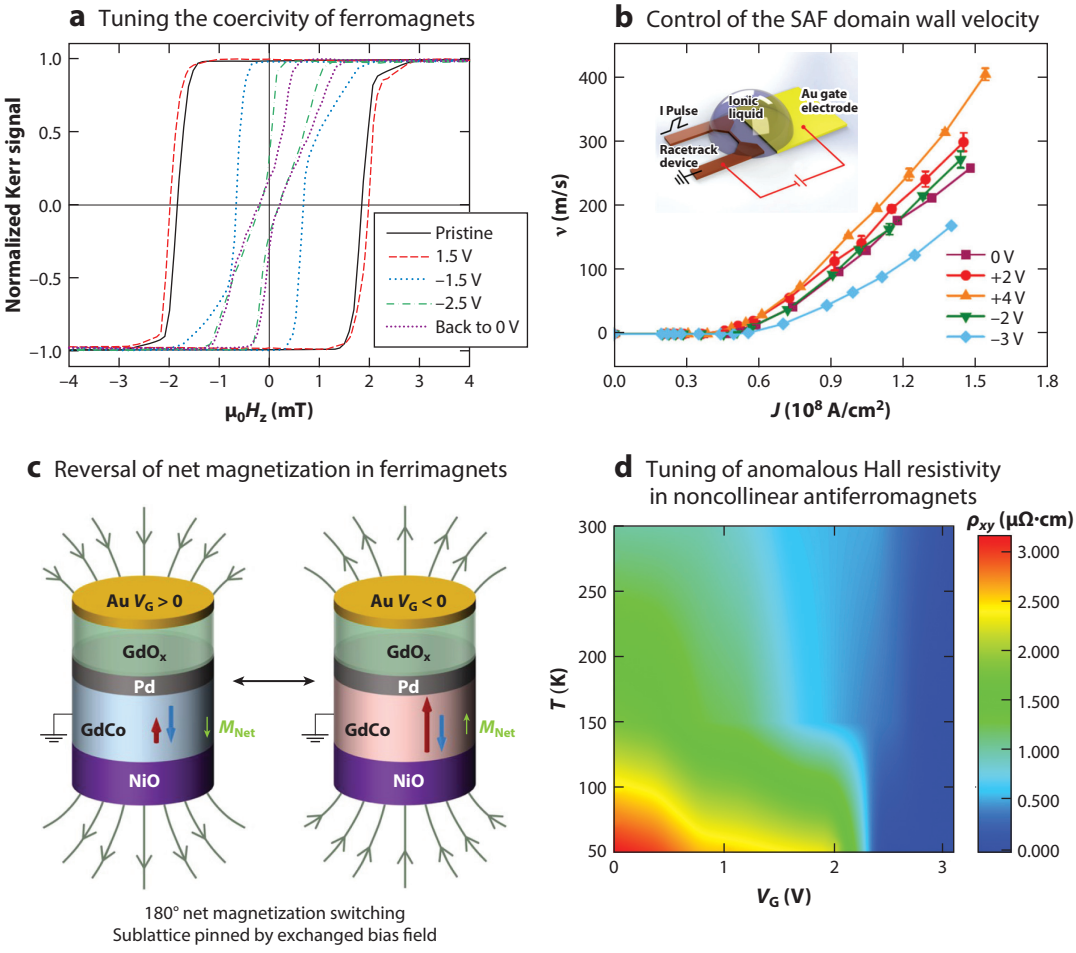

Figure 3

Examples of magneto-ionic research on magnetic metallic thin films. (*a*) Magnetic field H_z dependence of the normalized Kerr signal for the Pt/Mn_2CoAl system for different gate voltages applied by an ionic liquid. Panel adapted from Reference 99; copyright 2021 American Physical Society. (*b*) Ionic liquid gate control of synthetic antiferromagnetic (SAF) domain wall velocity versus injected current density; the inset shows a schematic illustration of ionic liquid gating on a magnetic racetrack device. Panel adapted from Reference 88; copyright 2021 Springer Nature. (*c*) Schematic illustration of a device layer structure demonstrating deterministic 180° voltage-controlled reversal of net magnetization when the ferrimagnetic GdCo layer is loaded (*left*) and unloaded (*right*) with hydrogen in the structure NiO/Pd/GdCo/Pd with an Au/GdO_x gate. Panel adapted with permission from Reference 47; copyright 2021 Springer Nature. (*d*) Ionic liquid gate voltage–dependent contour mapping of anomalous Hall resistivity ranging from 50 to 300 K in the noncollinear antiferromagnetic Mn_3Ge/Al_2O_3. Panel adapted with permission from Reference 100; copyright 2022 Wiley.

exchange coupled but the exchange coupling between the sublattices is antiferromagnetic. The net magnetization, that is, the degree to which the sublattice magnetizations are different, allows the state of the ferrimagnet to be easily detected (unlike antiferromagnets, which possess no net magnetization). This net moment, depending on the specific system, can often be manipulated by temperature, magnetic field, or materials engineering approaches. Furthermore, the smaller net magnetization gives rise to significantly faster magnetization dynamics. For these reasons, ferrimagnetic systems are very interesting for spintronics applications (104–110).

Perhaps the archetypical metallic ferrimagnetic materials system is that of alloys formed from one or more rare earth (RE) elements (e.g., Gd, Tb) and one or more transition metal (TM) elements (e.g., Co, Fe), such as GdCo, GdFeCo, and FeTb. These systems have been studied in various contexts for decades (105, 107–110). The structure of these alloys is typically amorphous, and the RE and TM elements form ferromagnetically aligned sublattices, the moments of which are oriented antiparallel to each other. Since the magnetization of the RE sublattice varies much more strongly with temperature than that of the TM, there is typically a so-called magnetization compensation temperature where the two sublattices have exactly equal and opposite moments such that the net magnetic moment at this temperature is zero. These systems have been extensively explored in multiple contexts ranging from magneto-optical recording and magnetization dynamics to spin transport, but voltage control of such systems has been little developed to date. Recently, by using a solid-state electrolyte gate formed from GdO_x/Au, Huang et al. (47) realized the magneto-ionic manipulation of the ferrimagnetic order in a Pt/GdCo/Pd thin-film structure. Under a positive gate voltage, the gate catalyzes water dissociation sourced from ambient humidity and thereby injects protons into the GdCo layer, while a negative gate voltage enables proton extraction. Such hydrogen loading and unloading results in a sizable change in the magnetic moment of the Gd sublattice while allowing for a much smaller change in the Co sublattice moment, resulting in the controlled switching of the dominant sublattice between the Gd and Co sublattices. Gating in this way also results in a significant shift of over 100 K in the compensation temperature while a voltage-controlled deterministic 180° magnetization reversal is realized in the absence of any external magnetic field (**Figure 3*c***). Huang et al. (47) further utilized gate-controlled localized moment switching for the generation of domain walls and skyrmions, which are of potential interest for realizing magneto-ionic solid-state memory and logic functions. Wang et al. (111) reported nonvolatile changes in the coercive field, anomalous Hall resistance, and compensation temperature in GdFeCo ferrimagnetic thin films by ionic liquid gating. They showed that the compensation temperature can be modified by as much as 29 K for a gate voltage of −4 V, which they attributed to the redox reaction of the active Gd element with oxygen ions from the ionic liquid. These initial studies have demonstrated that a magneto-ionic approach is interesting for the manipulation of ferrimagnetic systems, especially considering the different chemical reaction activities of the RE and TM sublattices.

4.4. Antiferromagnetic Metallic Films

Antiferromagnetic systems are of great theoretical interest, but detecting their magnetic configuration is nontrivial due to the absence of any net magnetization, which makes their use in applications more challenging (104, 106). One important use for antiferromagnets is that they can give rise to an offset field in the magnetization versus magnetic field hysteresis loop of a ferromagnetic layer (or nanoparticle) that is in direct contact to an antiferromagnet. This is known as an exchange bias field. Exchange bias has been used in magnetic sensors to set the direction of a magnetic layer either locally, as in sensors based on anisotropic magnetoresistance, or globally, as in spin-valve sensors based on the giant magnetoresistance effect (112). The voltage control of exchange bias could be highly useful in the development of low-energy-consumption spintronic memory devices (113). Magneto-ionic control of exchange bias via oxygen ion migration has been demonstrated in several systems such as IrMn/Fe/FeO_x and Pt/Co/Ni/HfO_2 (45, 114). In both of these systems, the oxygen ions in the oxide electrolyte migrate into or away from the ferromagnetic layer and influence its oxidation level. Such a redox-based chemical reaction will change the effective thickness of the ferromagnetic layer and thus the saturation magnetization and perpendicular magnetic anisotropy, which in turn influences the exchange bias. Zehner

et al. (48) recently reported magneto-ionic control of exchange bias in NiO/Pd/Co/Pd via proton pumping using a solid gate of $Gd(OH)_3$/Au. The loading and unloading of protons in the Pd/Co/Pd system affect the perpendicular magnetic anisotropy and therefore influence the exchange bias, which can be achieved by applying a sequence of voltage and magnetic fields (48).

Apart from exchange bias, the potential of antiferromagnetic systems themselves for realizing low-energy-consumption and high-speed spintronic devices has attracted much attention in recent years. It has been claimed that the Néel vector in the collinear antiferromagnets CuMnAu and Mn_2Au can be reversed via novel local spin–orbit torques generated by an electric current passing through the materials' layers (106, 115, 116). However, these claims have recently been challenged (117, 118), and the role of temperature-induced resistive switching (i.e., nonmagnetic effects) was shown to be dominant. Studies have explored the magneto-ionic control of these collinear antiferromagnets, but the effects were weak compared with voltage control manipulation via, for example, ferroelastic strain from a piezoelectric substrate (116).

In addition to collinear antiferromagnets, noncollinear, chiral antiferromagnets such as the Mn_3X (X = Sn, Ge, Ga, Pt) system have also attracted much attention since they exhibit large anomalous Hall signals even with negligible magnetization (119, 120). The large anomalous Hall signal has an intrinsic origin from the Berry curvature derived from the electronic band structure of these Weyl semimetals (119, 120). Such exotic properties make these noncollinear, chiral antiferromagnets very interesting prospective candidates for information encoding. Qin et al. (100) successfully realized ionic liquid gate control of the anomalous Hall resistivity of ultrathin Mn_3Ge films. They found that they could switch off the anomalous Hall resistivity under positive gate voltages at various temperatures (**Figure 3*d***). They claimed an electrostatic origin since the changes in the anomalous Hall resistivity were found to be volatile and argued that changes in the carrier density of such thin films via electrostatic doping changes the chemical potential, which subsequently switches off the anomalous Hall effect (100). It is very unusual that the electrostatic gating of a good metal can significantly modify the carrier density to have much effect, but this work nevertheless raises the questions of whether a magneto-ionic approach for manipulating the properties of noncollinear antiferromagnets is feasible and what the detailed underlying mechanism is. The rich physics and tantalizing prospects for applications make antiferromagnetic systems promising platforms for future spintronics research using magneto-ionic approaches.

5. IONIC GATE TUNING OF 2D VAN DER WAALS MATERIALS

The family of 2D van der Waals (vdW) materials, which are layered materials that possess anisotropic bonding with strong covalent bonds within the plane and weak vdW bonds perpendicular to the plane, has received enormous interest in recent years because they exhibit unique physical properties as compared with their 3D counterparts. Such properties include continuous phase transitions, quantum metallic states, and localization of electrons (121). Since the first experiments on graphene (122), there has been an extremely rapid increase in the family of 2D vdW materials studied, including metals (e.g., $NbSe_2$), semiconductors (e.g., MoS_2), and insulators (e.g., hexagonal boron nitride) (123–125). Electric-field effects have been widely used to tune the physical properties of large numbers of 2D vdW materials, such as their IMTs, superconductivity, and magnetism, as well as to mimic synaptic plasticity for neuromorphic computing devices (37, 123, 124, 126–128). In the following sections, ionic gate control, especially using the electrochemical approach, of superconductivity and magnetism in 2D vdW materials, including TM dichalcogenides (TMDs), honeycomb bilayer superconductors, and 2D ferromagnetic materials, is briefly introduced.

5.1. Ionic Gate Tuning of Superconductivity in 2D van der Waals Materials

Since the first groundbreaking work on thin-film superconductivity in 1938 (129), 2D superconductivity has been intensively studied. Thanks to significant developments in the methods used to prepare 2D superconducting materials, the crystallinity of 2D films has greatly improved, and the preparation of single- or few-atom-thick layers has been achieved (123, 130). Such improvements have enabled access to superconductivity at the 2D limit as well as provided for a platform for searching for new physics, including attempts to realize the holy grail of room temperature superconductivity. TMDs with the formula MX_2 (where M is a TM and X is a chalcogen) are a family of 2D vdW layered materials that offer a wide range of electronic properties. Since electrons are largely confined within the covalently bonded layers, intrinsic 2D superconducting features can be expected from a TMD monolayer. An extremely interesting characteristic is Ising superconductivity, which has recently been observed in several TMDs including MoS_2, WS_2, TaS_2, and $NbSe_2$ (123, 124, 131, 132). The in-plane upper critical magnetic fields of these Ising superconductors are far larger than the Pauli limit as a result of an Ising spin–orbit coupling that pins the electron spins to the out-of-plane direction and thereby prevents the electron spins within the Cooper pairs from being polarized in-plane (123, 124, 131, 132). Ionic gating approaches are perfectly suited to manipulating the properties of single- or few-monolayer vdW systems since very large changes in 2D carrier densities are possible at this atomic limit. This method has been widely used in TMD systems to trigger electronic phase transitions, including transitions into a superconducting state as in, for example, studies on the gating of thin flakes of MoS_2 with the 2H-type crystal structure (124). Using a dual-gate configuration composed of an ionic liquid top gate and a solid back gate with an HfO_2 dielectric layer, the continuous modulation of the carrier density below superconducting ordering temperature T_C was explored by first approaching the quantum critical point of superconductivity via ionic liquid gating and then tuning this superconducting state using conventional back gating. The latter results in a continuous increase in the T_C of MoS_2 (124).

In addition to the voltage control of superconductivity in 2D vdW materials via electrostatic doping, electrochemical processes can also be utilized. The ionic gate–induced manipulation of the 2D vdW Ising superconductor WS_2, which possesses highly interesting properties such as superior Ising protection and a second insulating state subsequent to the superconducting dome (131, 133), has been extensively explored. The superconducting phase has been realized in WS_2, and its T_C has been enhanced up to 8.6 K via reversible electrochemical doping with K^+ ions using an electrolyte medium of $KClO_4$ and polyethylene glycol. This process results in a K^+-intercalated compound, K_xWS_2, which is superconducting over a range of K^+-intercalation for x values from ∼0.05 to ∼0.2. Interestingly, while T_C varies under different gate voltages in MoS_2, the T_C in WS_2 is fixed under various gate voltages and disappears when a dominating, nonsuperconducting state appears after overdoping with potassium above $x \approx 0.4$ (133). In the work of Yoshida et al. (134), the voltage control of T_C in $NbSe_2$ shows both reversible and irreversible changes as the gate voltage is varied. In the high-voltage regime, where electrochemical processes are dominant, an irreversible decrease of T_C is associated with chemical etching of the film. In the work of Hitz et al. (135), however, through electrochemical processes based on Li^+ ion intercalation, the superconductivity in $NbSe_2$ can be readily manipulated by ionic liquid gating: $NbSe_2$ shows a lower T_C under zero voltage than does pristine $NbSe_2$, which is regarded to be a result of the spontaneous intercalation of Li^+ ions into the vdW gaps. A nonmonotonic increase of T_C with decreasing negative voltage is also observed due to the competition between the extraction of Li^+ and intercalation of ClO_4^- (134, 135). Research on the vdW material $SnSe_2$ has confirmed that Li^+ ions are driven in between the $SnSe_2$ layers and form a single reservoir layer that provides electrons and that, thereby, enhances T_C up to 4.8 K (136). Another example is thin flakes of 1T-TaS_2 (**Figure 4*a–c***), in which ionic gating at low temperatures induces multiple phase

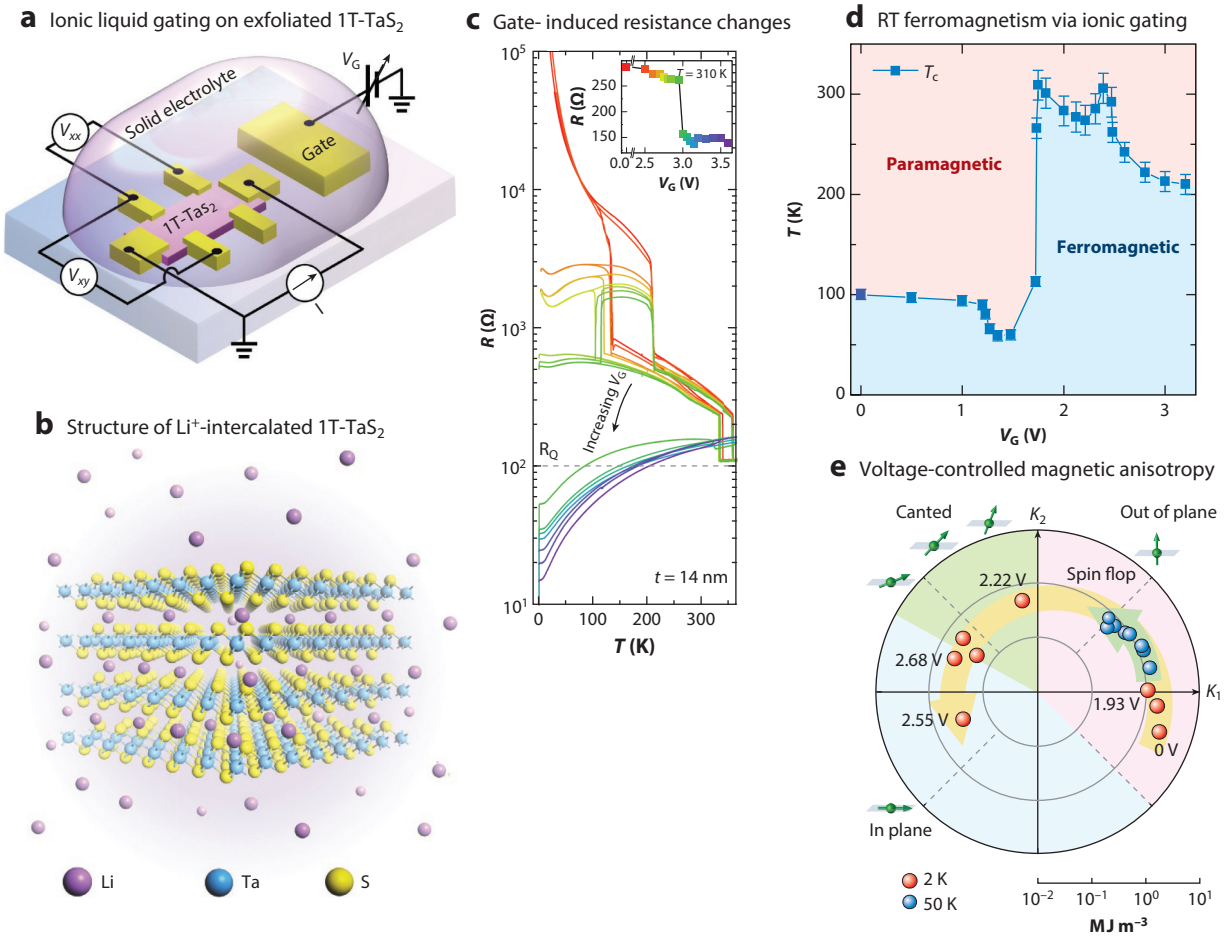

Figure 4

Examples of ionic gate–induced tuning of physical properties in 2D van der Waals materials. (*a*) Schematic illustration of ionic gating of an exfoliated 1T-TaS_2 flake. (*b*) Side view of the 1T-TaS_2 crystal structure with ionic gate–induced Li^+ ion intercalation. (*c*) Temperature-dependent resistance at fixed gate voltages for a 14-nm-thick 1T-TaS_2 flake. The inset, which serves as a color-coded reference of gate voltage, displays the gate-induced electronic phase transition between nearly commensurate and incommensurate charge-density wave states at 310 K. (*d*) Phase diagram of a trilayer Fe_3GeTe_2 sample as the gate voltage V_g and temperature are varied, revealing room temperature (RT) ferromagnetism via ionic liquid gating. (*e*) Polar chart of gate voltage–dependent magnetic anisotropic energy of a Fe_5GeTe_2 flake with a thickness of 23 nm at 2 K (*red dots*) and 50 K (*blue dots*). Panels *a–c* adapted with permission from Reference 34; copyright 2015 Springer Nature. Panel *d* adapted with permission from Reference 127; copyright 2018 Springer Nature. Panel *e* adapted with permission from Reference 139; copyright 2022 Springer Nature.

Erratum >

transitions from a Mott insulator to a metal, with a five-orders-of-magnitude change in resistance and superconductivity finally emerging in a textured charge-density wave state (34). Note that the voltage-controlled intercalation of Li^+ and Na^+ ions has been widely used to manipulate superconductivity in other 2D materials such as flakes of the iron-based superconductor FeSe and honeycomb bilayer superconductors (137, 138).

Ionic gating manipulation of the honeycomb bilayer superconductor has been realized for the archetypical band insulator ZrNCl. The honeycomb bilayer structure is formed as follows: Three $(ZrNCl)_2$ monolayers bonded by vdW interactions form a unit cell of ZrNCl, while the double

honeycomb $(ZrN)^+$ layers are sandwiched by two Cl^- layers in each monolayer. A strong covalent interaction exists within the $(ZrN)^+$ double layer in comparison with the relatively weak interaction between the $(ZrN)^+$ and Cl^- layers. In contrast to the chemically doped bulk case, where phase separation is commonly observed, electrochemical gating of ZrNCl can tune the superconductivity while circumventing phase separation (138). Ionic liquid gated Li_xZrNCl shows superconductivity in the low carrier density regime down to $x = 0.0038$ with the highest T_C, 19.0 K, for $x = 0.011$. In other honeycomb bilayer superconductors, such as ZrNCl, HfNCl, and ZrNBr, the highest T_C induced by electrochemical gating is ∼24.9 K for HfNCl (140). When high gate voltages are applied, a highly temperature-sensitive reversible gate-induced insulator–superconductor transition is observed in these materials. The most astonishing finding is that by continuously decreasing the amount of Li^+ ion intercalation in ZrNCl, a monotonic increase of the dimensionless coupling strength Δ/E_F (where Δ is the superconducting gap and E_F the Fermi energy) above 0.3 is observed, indicating a voltage-controlled crossover between a Bardeen–Cooper–Schrieffer state and a Bose–Einstein condensation state.

5.2. Magnetism in 2D van der Waals Materials

Despite the vast range of physical phenomena exhibited by 2D vdW materials, until recently, magnetic systems have been less explored, even though layered and vdW bonded magnetic crystals have been available for some time. There are many promising avenues for research into magnetic 2D vdW materials, especially including heterostructures that combine different vdW materials, such as materials with distinct magnetic orders or the combination of a magnetic vdW material with a superconducting vdW material or ferroelectric vdW material. Another highly interesting avenue for exploration is gating with intense electric fields.

The search for 2D vdW magnetic materials is often conducted via exfoliation from a bulk layered parent compound that is magnetic (141). Due to the Mermin–Wagner–Hohenberg theorem, long-range magnetic order cannot be sustained at the 2D limit (142), so there is no guarantee of long-range 2D magnetism when decreasing the material dimensions from 3D to 2D. The presence of magnetic anisotropy, however, can overcome this fundamental obstacle. Strong spin–orbit coupling can give rise to significant magnetic anisotropy and, thereby, allow for the realization of 2D magnetic order (127, 128, 143). The first experimental confirmation of magnetism in 2D vdW materials was observed in monolayer CrI_3 and bilayer $CrGeTe_3$ (128, 143, 144). For the case of $CrGeTe_3$, the magnetism does not survive to the monolayer limit due to the absence of magnetic anisotropy (144); for the case of CrI_3, on the other hand, the existence of spin–orbit coupling helps magnetism to survive even down to the monolayer limit (143). This has also been demonstrated for monolayers of $CrCl_3$ that were prepared by molecular beam epitaxy (145).

Studies of the thickness dependence of the magnetic ordering in CrI_3 revealed an antiferromagnetic coupling between the ferromagnetically ordered monolayers. These studies showed that the magneto-optical Kerr signal disappears when varying the layer number from 1 to 2 and reappears when the layer number is further increased to 3 (143). The antiferromagnetic coupling at the 2D limit was unexpected as CrI_3 is ferromagnetic in the bulk case. These different behaviors between bulk and one- to few-layer-thick vdW materials highlight the reasons for extreme interest in these materials.

The effect of electric fields on the magnetism of few-layer-thick CrI_3 has been explored in a dual-gate configuration with solid gates. Electrostatic doping can readily manipulate the magnetization, coercive field, and Curie temperature in monolayer CrI_3, with a corresponding enhancement or diminishment enabled by hole or electron doping, respectively. In the bilayer CrI_3 case, electrostatic doping was found to introduce a reversible change in the coupling between the

antiferromagnetic and ferromagnetic interlayers (128). With the aid of a fixed applied magnetic field, voltage-controlled switching of the bilayer CrI_3 was realized, which is very interesting for future spintronic devices based on 2D vdW materials.

The presence of magnetism at the monolayer limit was later observed in exfoliated flakes of the 2D ferromagnet Fe_3GeTe_2 and its siblings with different iron compositions (127, 139). The metallic nature of this material has enabled the investigation of its magnetism using the anomalous Hall effect. The uniqueness of 2D ferromagnetism in Fe_3GeTe_2 is related to two thickness-dependent transitions. The first is that the magnetic hysteresis loop exhibits a perfect rectangular shape with ultrasharp switching at corresponding coercive fields in thin Fe_3GeTe_2 films, while in the thick regime, the magnetic hysteresis loop possesses a more complex shape, and labyrinthine magnetic domains are observed (127). The second thickness-dependent transition is that from a 3D Heisenberg ferromagnet to a 2D Ising ferromagnet when shrinking the thickness of a Fe_3GeTe_2 film from the bulk to the monolayer limit. Electric-field effects have also been used to investigate the 2D magnetic properties of Fe_3GeTe_2, but by using an ionic gating approach (127). With a Li-based electrolyte, the Curie temperature of a trilayer Fe_3GeTe_2 film under increasing positive gate voltage increases from 100 K at the pristine state to above room temperature but then decreases with further increases in gate voltage (**Figure 4*d***). The coercive field also shows a nonmonotonic response to increasing gate voltage at a fixed temperature. A proposed interpretation is that Li^+ ion intercalation by ionic gating induces a substantial shift of the electronic bands in Fe_3GeTe_2. Therefore, such an increase in the density of states at the Fermi level fulfills the Stoner criterion of itinerant ferromagnetism and thus realizes room temperature 2D ferromagnetism (127). Such a model of Li^+ ion intercalation also accounts for the results of a very recent study of ionic gate–induced magnetic anisotropy in Fe_5GeTe_2 (139) (**Figure 4*e***). To conclude, the ionic gating approach has proven to be very effective in manipulating 2D magnetism and is worthy of further investigation.

6. NEUROMORPHIC COMPUTING VIA IONIC GATING

Modern von Neumann computing architectures suffer from large energy consumption needs and high latency of data transmission due to serial data processing and the separation of data storage and processing. One approach to next-generation computing systems that could circumvent these bottlenecks and allow for higher energy efficiency is neuromorphic computing, which allows for the integration of data processing and memory (146). Neuromorphic computing concepts are inspired by the massive parallelism, robust computation, and efficiency of the human brain. In the brain, pre- and postsynaptic neurons are connected via massive numbers of adaptive synaptic connections. These act as a complete processor in which data are stored as tunable strengths of synaptic connections. Incoming signals (action potentials) from the presynaptic neurons travel along axons and across the synapses via neurotransmitters to the postsynaptic neurons. Different types of neural functions can be triggered depending on the spatiotemporal differences between the incoming signals and the plasticity of the synaptic connections (146).

Concerning the timescale of activity variations, synaptic plasticity can be classified into two main types: short term and long term. In short-term synaptic plasticity, a temporal enhancement of a synaptic connection quickly decays to its initial state on a timescale of milliseconds to a few minutes; such temporal and spatial characteristics of neural activity can be realized by enhancing the synaptic transmission in a controllable manner. In long-term synaptic plasticity, the enhancement of the synaptic connection is maintained on a much longer timescale, from minutes to hours or even permanently, and has thus been widely considered the biological basis for long-term learning and memory. Artificial synapses with both short- and long-term plasticity can be emulated using

an ionic gating approach through combinations of electrostatic and electrochemical processes that consider their respective volatile and nonvolatile natures. This makes ionic gating potentially highly useful for achieving the tunability needed for neuromorphic computing (37, 38, 147–149). An artificial synapse based on an ionic gate–controlled phase transition is as follows: The gate contact acts as the terminal from the presynaptic cell, while the drain and source contacts act as the postsynaptic cell. When no gate voltage is applied, the channel between the source and the drain is highly resistive or even insulating, leading to a very low or diminished current. With increasing gate voltage, an ionic gate–controlled electronic phase transition takes place, thereby modulating the conductance of the channel and allowing for the transmission of high current. As a result, gate voltages with different frequencies and amplitudes are equivalent to the stimuli from the presynaptic cell and thus trigger different action potentials (current flows through the source and drain) in the postsynaptic cell.

The ionic gating approach, as introduced in Sections 3, 4, and 5, has significant advantages with respect to mimicking synaptic plasticity as it can tune the properties of materials with high precision and reversibility as well as in multiple analog steps. Moreover, the nonvolatility of the ionic gating approach enables decoupling of data programming and storage processes, which leads to both low-power switching and good retention properties. The most widely used material system for building an artificial synapse is VO_2, as it can be grown with high crystalline quality on different substrates and can exhibit a well-defined insulator-to-metal phase transition that can be manipulated through multiple methods such as with an electric field or by thermal or even optical control. These crucial characteristics have made VO_2 an ideal material platform for emulating artificial synapses with high reliability, scalability, and stability (147, 148). In the work of Deng et al. (147), utilizing an ionic gel gate, a VO_2 Mott transistor deposited on a mica substrate was developed to simulate the functions of a biological synapse with tunable short-term and long-term plasticity realized by gate voltage–induced volatile electrostatic carrier accumulation and nonvolatile proton doping (**Figure 5*a–c***). Deng et al. (147) successfully simulated an important sensory neuron, the nociceptor, by achieving multiple essential synaptic functions in a synaptic transistor with key characteristics of threshold, relaxation, and sensitization. Such a synaptic transistor exhibits superior stability with a high tolerance to exterior mechanical forces. Simulation results demonstrated a high recognition accuracy for handwritten digits (>95%) in a convolution neural network built from these synaptic transistors (147). In the work of Li et al. (148), by combining an electrochemical gating method and ultraviolet irradiation, nonvolatile multilevel control of VO_2 films by oxygen stoichiometry engineering was realized. Based on this reversible regulation of VO_2 films using ultraviolet irradiation and ionic gating, Li et al. (148) demonstrated a proof-of-principle neuromorphic ultraviolet sensor with integrated sensing, memory, and processing functions at room temperature and also proved its silicon-compatible potential through the wafer-scale integration of a neuromorphic sensor array. The device displayed linear weight updates via optical writing because the metallic phase proportion increases almost linearly with the light dosage. Moreover, the artificial neural network consisting of this neuromorphic sensor can extract information from the surrounding environment that is carried by ultraviolet light and can significantly improve recognition accuracy from 24% to 93% (148).

In addition to neuromorphic computing devices built with VO_2, there has also been a plethora of work on emulating synapses using ionic gate–induced intercalation of Li^+ and Na^+ ions in the family of 2D materials (37, 38, 149, 150). In the few-layer graphite system, room temperature voltage control of Li^+ ion intercalation was used to develop a graphene-based synapse with ultrafast switching speeds (150). A decoupling of the writing and reading processes was realized through turning on and off the gate voltage during the writing and reading process, respectively. This is due

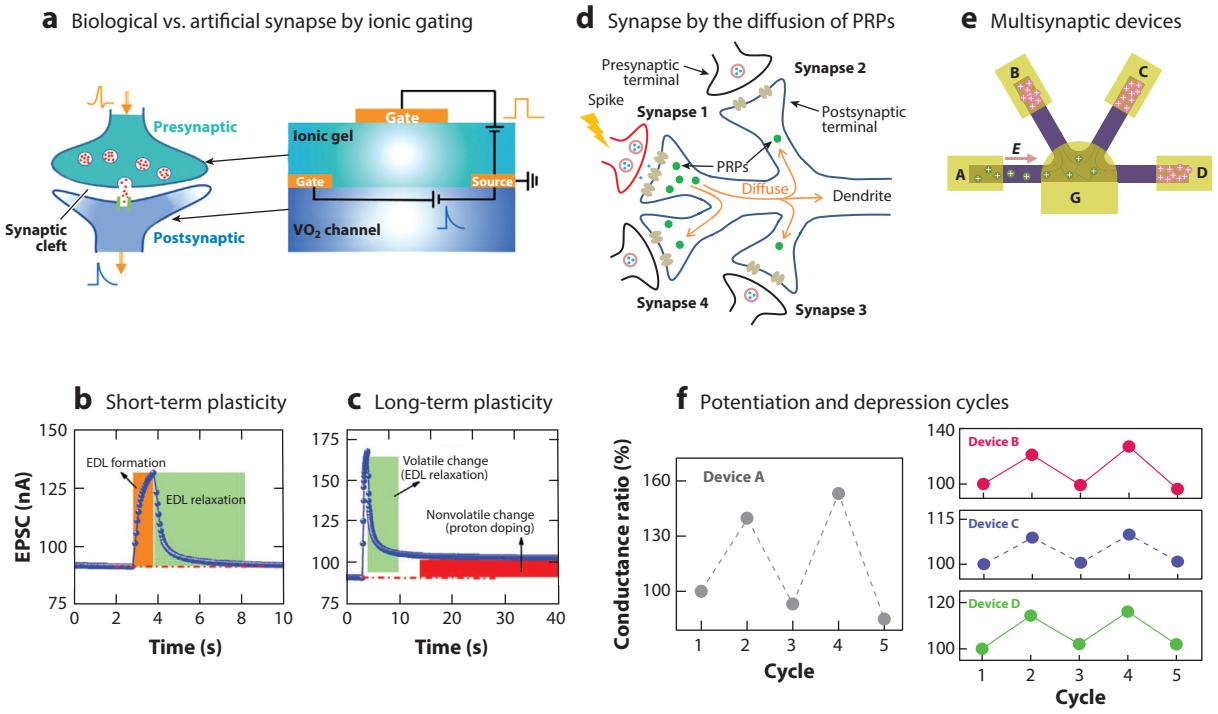

Figure 5

Examples of artificial synapses based on ionic field-effect transistors. (*a*) Schematic illustration of a biological chemical synapse composed of a presynaptic membrane, synaptic cleft, and postsynaptic membrane and the corresponding artificial synapse formed from an electrolyte-gated VO_2-channel Mott transistor. (*b*) Short-term and (*c*) long-term plasticity via monitoring the EPSC in the VO_2-based synapse for different gate voltages. (*d*) A schematic showing synaptic interactions enabled by the diffusion of PRPs among multiple synapses and (*e*) the corresponding multisynaptic device formed from MoS_2. (*f*, *left*) Potentiation and depression cycles of device A in the multisynaptic device shown in panel *e* and (*f*, *right*) the corresponding conductance changes in nonstimulated devices B, C, and D when device A was potentiated or depressed. Panels *a–c* adapted with permission from Reference 147; copyright 2021 Wiley. Panels *e–f* adapted with permission from Reference 37; copyright 2019 Spring Nature. Abbreviations: EDL, electric double layer; EPSC, excitatory postsynaptic current; PRPs, plasticity-related proteins.

to the nonvolatile nature of the electrochemical approach as the states of synapses can be maintained when the gate voltage is turned off. The synapse thus exhibits a low power consumption of less than 500 fJ per switching event and analog tunability between more than 250 nonvolatile states, as well as good endurance and retention behavior (more than 6,000 pulses). This work is significant for the development of multifunctional neuromorphic computing systems, especially considering the compatibility of graphene with today's complementary metal oxide semiconductor architecture (150). Yang et al. (149) reported an all-solid-state electrochemical transistor made with a Li^+ ion–based solid dielectric and 2D α-phase MoO_3 nanosheets that form the channel. Through reversible intercalation of Li^+ ions into the α-MoO_3 lattice, a nonvolatile conductance modulation in an ultralow conductance regime is achieved in these devices. Based on this operating mechanism, some essential functionalities of synapses, such as short- and long-term synaptic plasticity and bidirectional near-linear analog weight updates, were demonstrated. Simulations using handwritten digit data sets were used to demonstrate the high recognition accuracy (94.1%) of the synaptic transistor arrays.

The TMDs can also be utilized to emulate synapses by intercalating ions into the vdW gap or by ion intercalation–induced structural changes (37, 38). Artificial synapses fabricated from thin films of the vdW material WSe_2 exhibit comparable performance to that of a biological synapse, with a diversity of short-term and long-term plasticity including excitatory postsynaptic current, paired pulse facilitation, spiking-rate dependent plasticity, and dynamic filtering; such devices also possess ultralow energy consumption (~30 fJ) and remarkable linearity and symmetry of their resistance response. Zhu et al. (38) also carried out a detailed transmission electron microscopy characterization and ab initio calculations to reveal the underlying mechanisms that accounted for the observed short- and long-term plasticity. They find that these are a result of surface absorption and internal intercalation in the WSe_2 vdW gap, which causes different poststimulation diffusion dynamics. An effective manipulation of synaptic activity is then carried out via tailoring the electrochemical gating and consequent diffusion dynamics by varying the thickness and structure of the vdW materials as well as the number, duration, rate, and polarity of gate simulations, which show the diversity of artificial synapses emulated by vdW materials for low-power neuromorphic systems (38). In the MoS_2 thin-film system, ionic gating can result in a reversible electronic phase transition between a semiconducting and a metallic phase due to a local structural (2H–1T′) phase transition resulting from Li^+ ion redistributions. Such a modulation leads to reliable memristive behavior in MoS_2-based synaptic devices. In addition, the high in-plane diffusivity of Li^+ ions in turn allows for efficient ionic coupling of multiple MoS_2 devices (**Figure 5*d–e***) and provides a mechanism for implementing synaptic competition and synaptic cooperation effects in bioinspired artificial neural networks (37). These results demonstrate that ionic gate–controlled synaptic transistors formed from vdW materials are promising candidates for the exploitation of neuromorphic systems with complex functions in the future.

7. FUTURE PROSPECTS AND CHALLENGES

This review covers recent progress in the ionic gate control of material properties of diverse systems, particularly changes in properties resulting from an electrochemical mechanism, namely the electric field–induced migration of ions. Even though electrostatic doping mechanisms show potential for enabling relatively fast, reversible, and reproducible changes in the properties of the gated material, a strong limitation of this approach is its highly interfacial nature because it is limited by the penetration depth of the gating electric field. Electrochemical processes, on the contrary, can go well beyond an interfacial region due to the electric field–induced migration of diverse ionic species, which is driven by chemical potential gradients as the ionic species are added to or removed from a region close to the ionic gate and channel region, resulting in phase transformations of materials. A highly useful aspect of the electrochemical approach is that it can be nonvolatile. The ionic gating approach has been proven to be highly effective in modulating many structural, electronic, magnetic, and superconducting properties of various material systems, including TM oxides, magnetic metallic thin films, and 2D vdW materials. Multiple new physical phenomena have been revealed from electrochemical-induced changes in diverse materials, and a variety of functional devices have been realized or proposed that suggest paths toward real applications, especially toward the building of neuromorphic computing devices and systems of devices. However, there still remain many open questions and challenges, which make this field of research highly interesting.

One basic question lies in the detailed mechanisms that underlie ionic gating. Both the electrostatic and electrochemical processes accompany each other, so it is of great importance to understand the cooperation and competition between these two processes, especially with respect to the optimal device configuration, the preferred combinations of electrolytes and target

materials, and the voltages needed. There is already nascent research work focused on these issues, such as the real-time imaging of the migration of oxygen vacancies, but in the future, more experimental and theoretical approaches are needed to develop a thorough understanding. These will allow for the selective separation and combination of electrostatic and electrochemical processes, which will greatly benefit both material and functional device research.

Even though ionic gating approaches have attractive characteristics that are well suited for application-oriented computing architectures, such as neuromorphic computing, there remain highly interesting challenges, such as those involving response time and device size for large-scale integration. Very high response times using an electrochemically based ionic gating approach remain a challenge since the switching time is constrained by the ion mobility and chemical reaction times. Pursuing electrolyte materials with higher ion mobilities, modifying the target material structure, and designing improved device configurations are possible solutions for decreasing the response time. Solutions for device size and integration issues may come from developing technologies such as ion gel printing and patterning methods compatible with ionic liquids. In this regard, solid electrolytes and ionic conductors are appealing for developing highly scaled devices.

Newly emerging material systems, such as 2D vdW materials, are a fertile ground for exploring new physics through ionic gating methodologies. Compared with the vast amount of research on electronic phase transitions, work on electrochemically based ionic gating approaches is still limited, especially in the field of 2D ferromagnetism. The flourishing field of 2D vdW magnetic materials will very likely provide a broader platform for magneto-ionic approaches to bring about a wealth of intriguing fundamental science discoveries with a high potential for use in a range of applications.

To conclude, ionic gating allows for the voltage control of the properties of a very wide range of materials and thus shows great potential for realizing diverse categories of functional devices. A promising future can be foreseen for ionic gating in both fundamental research and real-world applications.

DISCLOSURE STATEMENT

The authors are not aware of any affiliations, memberships, funding, or financial holdings that might be perceived as affecting the objectivity of this review.

ACKNOWLEDGMENTS

This project has received funding from the European Union's Horizon 2020 Research and Innovation Program under grant agreement 737109.

LITERATURE CITED

1. Ahn CH, Triscone J-M, Mannhart J. 2003. Electric field effect in correlated oxide systems. *Nature* 424:1015–18
2. Ahn CH, Bhattacharya A, Di Ventra M, Eckstein JN, Frisbie CD, et al. 2006. Electrostatic modification of novel materials. *Rev. Mod. Phys.* 78:1185–212
3. Ramesh R, Schlom DG. 2008. Whither oxide electronics? *MRS Bull.* 33:1006–14
4. Chakhalian J, Millis A, Rondinelli J. 2012. Whither the oxide interface. *Nat. Mater.* 11:92–94
5. Hwang HY, Iwasa Y, Kawasaki M, Keimer B, Nagaosa N, Tokura Y. 2012. Emergent phenomena at oxide interfaces. *Nat. Mater.* 11:103–13
6. Matsukura F, Tokura Y, Ohno H. 2015. Control of magnetism by electric fields. *Nat. Nanotechnol.* 10:209–20
7. Weisheit M, Fähler S, Marty A, Souche Y, Poinsignon C, Givord D. 2007. Electric field-induced modification of magnetism in thin-film ferromagnets. *Science* 315:349–51

8. Chiba D, Fukami S, Shimamura K, Ishiwata N, Kobayashi K, Ono T. 2011. Electrical control of the ferromagnetic phase transition in cobalt at room temperature. *Nat. Mater.* 10:853–56
9. Ye J, Zhang YJ, Akashi R, Bahramy MS, Arita R, Iwasa Y. 2012. Superconducting dome in a gate-tuned band insulator. *Science* 338:1193–96
10. Costanzo D, Jo S, Berger H, Morpurgo AF. 2016. Gate-induced superconductivity in atomically thin MoS_2 crystals. *Nat. Nanotechnol.* 11:339–44
11. Kim SH, Hong K, Xie W, Lee KH, Zhang S, et al. 2013. Electrolyte-gated transistors for organic and printed electronics. *Adv. Mater.* 25:1822–46
12. Fujimoto T, Awaga K. 2013. Electric-double-layer field-effect transistors with ionic liquids. *Phys. Chem. Chem. Phys.* 15:8983–9006
13. Du H, Lin X, Xu Z, Chu D. 2015. Electric double-layer transistors: a review of recent progress. *J. Mater. Sci.* 50:5641–73
14. Bisri SZ, Shimizu S, Nakano M, Iwasa Y. 2017. Endeavor of iontronics: from fundamentals to applications of ion-controlled electronics. *Adv. Mater.* 29:1607054
15. Cho JH, Lee J, Xia Y, Kim B, He Y, et al. 2008. Printable ion-gel gate dielectrics for low-voltage polymer thin-film transistors on plastic. *Nat. Mater.* 7:900–6
16. Wang S, Ha M, Manno M, Frisbie CD, Leighton C. 2012. Hopping transport and the Hall effect near the insulator–metal transition in electrochemically gated poly(3-hexylthiophene) transistors. *Nat. Commun.* 3:1210
17. Yuan H, Shimotani H, Ye J, Yoon S, Aliah H, et al. 2010. Electrostatic and electrochemical nature of liquid-gated electric-double-layer transistors based on oxide semiconductors. *J. Am. Chem. Soc.* 132:18402–7
18. Jeong J, Aetukuri N, Graf T, Schladt TD, Samant MG, Parkin SS. 2013. Suppression of metal-insulator transition in VO_2 by electric field–induced oxygen vacancy formation. *Science* 339:1402–5
19. Li M, Han W, Jiang X, Jeong J, Samant MG, Parkin SS. 2013. Suppression of ionic liquid gate-induced metallization of $SrTiO_3$(001) by oxygen. *Nano Lett.* 13:4675–78
20. Yi HT, Gao B, Xie W, Cheong S-W, Podzorov V. 2014. Tuning the metal-insulator crossover and magnetism in $SrRuO_3$ by ionic gating. *Sci. Rep.* 4:6604
21. Bubel S, Hauser AJ, Glaudell AM, Mates TE, Stemmer S, Chabinyc ML. 2015. The electrochemical impact on electrostatic modulation of the metal-insulator transition in nickelates. *Appl. Phys. Lett.* 106:122102
22. Walter J, Wang H, Luo B, Frisbie CD, Leighton C. 2016. Electrostatic versus electrochemical doping and control of ferromagnetism in ion-gel-gated ultrathin $La_{0.5}Sr_{0.5}CoO_{3-\delta}$. *ACS Nano* 10:7799–810
23. Walter J, Yu G, Yu B, Grutter A, Kirby B, et al. 2017. Ion-gel-gating-induced oxygen vacancy formation in epitaxial $La_{0.5}Sr_{0.5}CoO_{3-\delta}$ films from in operando X-ray and neutron scattering. *Phys. Rev. Lett.* 1:071403
24. Perez-Muñoz AM, Schio P, Poloni R, Fernandez-Martinez A, Rivera-Calzada A, et al. 2017. In operando evidence of deoxygenation in ionic liquid gating of $YBa_2Cu_3O_{7-x}$. *PNAS* 114:215–20
25. Dong Y, Xu H, Luo Z, Zhou H, Fong DD, et al. 2017. Effect of gate voltage polarity on the ionic liquid gating behavior of $NdNiO_3/NdGaO_3$ heterostructures. *APL Mater.* 5:051101
26. Leng X, Pereiro J, Strle J, Dubuis G, Bollinger A, et al. 2017. Insulator to metal transition in WO_3 induced by electrolyte gating. *npj Quant. Mater.* 2:35
27. Schladt TD, Graf T, Aetukuri NB, Li M, Fantini A, et al. 2013. Crystal-facet-dependent metallization in electrolyte-gated rutile TiO_2 single crystals. *ACS Nano* 7:8074–81
28. Bruce PG, Saidi M. 1992. A two-step model of intercalation. *Solid State Ion.* 51:187–90
29. Lück J, Latz A. 2018. Modeling of the electrochemical double layer and its impact on intercalation reactions. *Phys. Chem. Chem. Phys.* 20:27804–21
30. Lu N, Zhang P, Zhang Q, Qiao R, He Q, et al. 2017. Electric-field control of tri-state phase transformation with a selective dual-ion switch. *Nature* 546:124–28
31. Cui B, Werner P, Ma T, Zhong X, Wang Z, et al. 2018. Direct imaging of structural changes induced by ionic liquid gating leading to engineered three-dimensional meso-structures. *Nat. Commun.* 9:3055
32. Han H, Sharma A, Meyerheim HL, Yoon J, Deniz H, et al. 2022. Control of oxygen vacancy ordering in brownmillerite thin films via ionic liquid gating. *ACS Nano* 16:6206–14

33. Zhang Q, He X, Shi J, Lu N, Li H, et al. 2017. Atomic-resolution imaging of electrically induced oxygen vacancy migration and phase transformation in $SrCoO_{2.5-\sigma}$. *Nat. Commun.* 8:104
34. Yu Y, Yang F, Lu XF, Yan YJ, Cho Y-H, et al. 2015. Gate-tunable phase transitions in thin flakes of 1T-TaS_2. *Nat. Nanotechnol.* 10:270–76
35. Wan CJ, Zhu LQ, Zhou JM, Shi Y, Wan Q. 2013. Memory and learning behaviors mimicked in nanogranular SiO_2-based proton conductor gated oxide-based synaptic transistors. *Nanoscale* 5:10194–99
36. van de Burgt Y, Lubberman E, Fuller EJ, Keene ST, Faria GC, et al. 2017. A non-volatile organic electrochemical device as a low-voltage artificial synapse for neuromorphic computing. *Nat. Mater.* 16:414–18
37. Zhu X, Li D, Liang X, Lu WD. 2019. Ionic modulation and ionic coupling effects in MoS_2 devices for neuromorphic computing. *Nat. Mater.* 18:141–48
38. Zhu J, Yang Y, Jia R, Liang Z, Zhu W, et al. 2018. Ion gated synaptic transistors based on 2D van der Waals crystals with tunable diffusive dynamics. *Adv. Mater.* 30:1800195
39. Sharbati MT, Du Y, Torres J, Ardolino ND, Yun M, Xiong F. 2018. Low-power, electrochemically tunable graphene synapses for neuromorphic computing. *Adv. Mater.* 30:1802353
40. Lee C, Lee J, Kim M, Woo J, Koo S-M, et al. 2019. Two-terminal structured synaptic device using ionic electrochemical reaction mechanism for neuromorphic system. *IEEE Electron Dev. Lett.* 40:546–49
41. Ji H, Wei J, Natelson D. 2012. Modulation of the electrical properties of VO_2 nanobeams using an ionic liquid as a gating medium. *Nano Lett.* 12:2988–92
42. Leng X, Bollinger A, Božović I. 2016. Purely electronic mechanism of electrolyte gating of indium tin oxide thin films. *Sci. Rep.* 6:31239
43. Jo M, Lee HJ, Oh C, Yoon H, Jo JY, Son J. 2018. Gate-induced massive and reversible phase transition of VO_2 channels using solid-state proton electrolytes. *Adv. Electron. Mater.* 28:1802003
44. Zhang H, Guo L, Wan Q. 2013. Nanogranular Al_2O_3 proton conducting films for low-voltage oxide-based homojunction thin-film transistors. *J. Mater. Chem. C* 1:2781–86
45. Zhou X, Yan Y, Jiang M, Cui B, Pan F, Song C. 2016. Role of oxygen ion migration in the electrical control of magnetism in Pt/Co/Ni/HfO_2 films. *J. Mater. Chem. C* 120:1633–39
46. Schott M, Bernand-Mantel A, Ranno L, Pizzini S, Vogel J, et al. 2017. The skyrmion switch: turning magnetic skyrmion bubbles on and off with an electric field. *Nano Lett.* 17:3006–12
47. Huang M, Hasan MU, Klyukin K, Zhang D, Lyu D, et al. 2021. Voltage control of ferrimagnetic order and voltage-assisted writing of ferrimagnetic spin textures. *Nat. Nanotechnol.* 16:981–88
48. Zehner J, Wolf D, Hasan M, Huang M, Bono D, et al. 2021. Magnetoionic control of perpendicular exchange bias. *Phys. Rev. Lett.* 5:L061401
49. Das A, Pisana S, Chakraborty B, Piscanec S, Saha SK, et al. 2008. Monitoring dopants by Raman scattering in an electrochemically top-gated graphene transistor. *Nat. Nanotechnol.* 3:210–15
50. Panzer MJ, Frisbie CD. 2006. High charge carrier densities and conductance maxima in single-crystal organic field-effect transistors with a polymer electrolyte gate dielectric. *Appl. Phys. Lett.* 88:203504
51. Xu H, Fathipour S, Kinder EW, Seabaugh AC, Fullerton-Shirey SK. 2015. Reconfigurable ion gating of 2H-$MoTe_2$ field-effect transistors using poly (ethylene oxide)-$CsClO_4$ solid polymer electrolyte. *ACS Nano* 9:4900–10
52. Misra R, McCarthy M, Hebard AF. 2007. Electric field gating with ionic liquids. *Appl. Phys. Lett.* 90:052905
53. Han H, Jacquet Q, Jiang Z, Sayed FN, Sharma A, et al. 2022. Hidden phases and colossal insulator-metal transition in single-crystalline T-Nb_2O_5 thin films accessed by lithium intercalation. arXiv:2203.03232v1 [cond-mat.mtrl-sci]
54. Lee J, Panzer MJ, He Y, Lodge TP, Frisbie CD. 2007. Ion gel gated polymer thin-film transistors. *J. Am. Chem. Soc.* 129:4532–33
55. Ueno K, Nakamura S, Shimotani H, Ohtomo A, Kimura N, et al. 2008. Electric-field-induced superconductivity in an insulator. *Nat. Mater.* 7:855–58
56. Ueno K, Nakamura S, Shimotani H, Yuan H, Kimura N, et al. 2011. Discovery of superconductivity in $KTaO_3$ by electrostatic carrier doping. *Nat. Nanotechnol.* 6:408–12

57. Bollinger AT, Dubuis G, Yoon J, Pavuna D, Misewich J, Božović I. 2011. Superconductor–insulator transition in $La_{2-x}Sr_xCuO_4$ at the pair quantum resistance. *Nature* 472:458–60
58. Nakano M, Shibuya K, Okuyama D, Hatano T, Ono S, et al. 2012. Collective bulk carrier delocalization driven by electrostatic surface charge accumulation. *Nature* 487:459–62
59. Yi D, Wang Y, van't Erve OMJ, Xu L, Yuan H, et al. 2020. Emergent electric field control of phase transformation in oxide superlattices. *Nat. Commun.* 11:902
60. Jeong J, Aetukuri NB, Passarello D, Conradson SD, Samant MG, Parkin SSP. 2015. Giant reversible, facet-dependent, structural changes in a correlated-electron insulator induced by ionic liquid gating. *PNAS* 112:1013–18
61. Passarello D, Jeong J, Samant MG, Parkin SSP. 2015. Depth-dependent giant lattice expansion of up to 5% in ionic liquid-gated 90 nm thick VO_2 (001)/Al_2O_3 ($10\bar{1}0$) films. *Appl. Phys. Lett.* 107:201906
62. Altendorf SG, Jeong J, Passarello D, Aetukuri NB, Samant MG, Parkin SSP. 2016. Facet-independent electric-field-induced volume metallization of tungsten trioxide films. *Adv. Mater.* 28:5284–92
63. Passarello D, Altendorf SG, Jeong J, Rettner C, Arellano N, et al. 2017. Evidence for ionic liquid gate-induced metallization of vanadium dioxide bars over micron length scales. *Nano Lett.* 17:2796–801
64. Zhang L, Zeng S, Yin X, Asmara TC, Yang P, et al. 2017. The mechanism of electrolyte gating on high-T_c cuprates: the role of oxygen migration and electrostatics. *ACS Nano* 11:9950–56
65. Li Z, Shen S, Tian Z, Hwangbo K, Wang M, et al. 2020. Reversible manipulation of the magnetic state in $SrRuO_3$ through electric-field controlled proton evolution. *Nat. Commun.* 11:184
66. Wang M, Sui X, Wang Y, Juan YH, Lyu Y, et al. 2019. Manipulate the electronic and magnetic states in $NiCo_2O_4$ films through electric-field-induced protonation at elevated temperature. *Adv. Mater.* 31:1900458
67. Saleem MS, Cui B, Song C, Sun Y, Gu Y, et al. 2019. Electric field control of phase transition and tunable resistive switching in $SrFeO_{2.5}$. *ACS Appl. Mater. Inter.* 11:6581–88
68. Song J, Chen Y, Chen X, Wang H, Khan T, et al. 2019. Tuning the magnetic anisotropy of $La_{2/3}Sr_{1/3}MnO_3$ by controlling the structure of $SrCoO_x$ in the corresponding bilayers using ionic-liquid gating. *Phys. Rev. Appl.* 12:054016
69. Song J, Chen Y, Chen X, Khan T, Han F, et al. 2020. Electric tuning of magnetic anisotropy and exchange bias of $La_{0.8}Sr_{0.2}CoO_3$/$La_{0.67}Sr_{0.33}MnO_3$ bilayer films. *Phys. Rev. Appl.* 14:024062
70. Zhang J, Zhou G, Yan Z, Ji H, Li X, et al. 2019. Interfacial ferromagnetic coupling and positive spontaneous exchange bias in $SrFeO_{3-x}$/$La_{0.7}Sr_{0.3}MnO_3$ bilayers. *ACS Appl. Mater. Inter.* 11:26460–66
71. ViolBarbosa C, Karel J, Kiss J, Gordan O-D, Altendorf S, et al. 2016. Transparent conducting oxide induced by liquid electrolyte gating. *PNAS* 113:11148–51
72. Passarello D, Altendorf SG, Jeong J, Samant MG, Parkin SSP. 2016. Metallization of epitaxial VO_2 films by ionic liquid gating through initially insulating TiO_2 layers. *Nano Lett.* 16:95475–5481
73. Hope MA, Griffith KJ, Cui B, Gao F, Dutton SE, et al. 2018. The role of ionic liquid breakdown in the electrochemical metallization of VO_2: an NMR study of gating mechanisms and VO_2 reduction. *J. Am. Chem. Soc.* 140:16685–96
74. Yoon H, Choi M, Lim T-W, Kwon H, Ihm K, et al. 2016. Reversible phase modulation and hydrogen storage in multivalent VO_2 epitaxial thin films. *Nat. Mater.* 15:1113–19
75. Ohno H, Chiba D, Matsukura F, Omiya T, Abe E, et al. 2000. Electric-field control of ferromagnetism. *Nature* 408:944–46
76. Chiba D, Kawaguchi M, Fukami S, Ishiwata N, Shimamura K, et al. 2012. Electric-field control of magnetic domain-wall velocity in ultrathin cobalt with perpendicular magnetization. *Nat. Commun.* 3:888
77. Shimamura K, Chiba D, Ono S, Fukami S, Ishiwata N, et al. 2012. Electrical control of Curie temperature in cobalt using an ionic liquid film. *Appl. Phys. Lett.* 100:122402
78. Ando F, Kakizakai H, Koyama T, Yamada K, Kawaguchi M, et al. 2016. Modulation of the magnetic domain size induced by an electric field. *Appl. Phys. Lett.* 109:022401
79. Koyama T, Nakatani Y, Ieda J, Chiba D. 2018. Electric field control of magnetic domain wall motion via modulation of the Dzyaloshinskii-Moriya interaction. *Sci. Adv.* 4:eaav0265
80. Hirai T, Koyama T, Obinata A, Hibino Y, Miwa K, et al. 2016. Control of magnetic anisotropy in Pt/Co system using ionic liquid gating. *Appl. Phys. Expr.* 9:063007

81. Parkin SSP, Hayashi M, Thomas L. 2008. Magnetic domain-wall racetrack memory. *Science* 320:190–4
82. Fukami S, Suzuki T, Nagahara K, Ohshima N, Ozaki Y, et al. 2009. Low-current perpendicular domain wall motion cell for scalable high-speed MRAM. In *2009 Symposium on VLSI Technology*, pp. 230–61. Piscataway, NJ: IEEE
83. Parkin S, Yang S-H. 2015. Memory on the racetrack. *Nat. Nanotechnol.* 10:195–98
84. Bader S, Parkin S. 2010. Spintronics. *Annu. Rev. Condens. Matter Phys.* 1:71–88
85. Tan AJ, Huang M, Avci CO, Büttner F, Mann M, et al. 2019. Magneto-ionic control of magnetism using a solid-state proton pump. *Nat. Mater.* 18:35–41
86. Reichel L, Oswald S, Fähler S, Schultz L, Leistner K. 2013. Electrochemically driven variation of magnetic properties in ultrathin CoPt films. *J. Appl. Phys.* 113:143904
87. Diez LH, Liu Y, Gilbert DA, Belmeguenai M, Vogel J, et al. 2019. Nonvolatile ionic modification of the Dzyaloshinskii-Moriya interaction. *Phys. Rev. Appl.* 12:034005
88. Guan Y, Zhou X, Li F, Ma T, Yang S-H, Parkin SSP. 2021. Ionitronic manipulation of current-induced domain wall motion in synthetic antiferromagnets. *Nat. Commun.* 12:5002
89. Yang Q, Wang L, Zhou Z, Wang L, Zhang Y, et al. 2018. Ionic liquid gating control of RKKY interaction in FeCoB/Ru/FeCoB and $(Pt/Co)_2/Ru/(Co/Pt)_2$ multilayers. *Nat. Commun.* 9:991
90. Zehner J, Soldatov I, Schneider S, Heller R, Khojasteh NB, et al. 2020. Voltage-controlled deblocking of magnetization reversal in thin films by tunable domain wall interactions and pinning sites. *Adv. Electron. Mater.* 6:2000406
91. Yamada K, Suzuki M, Pradipto A-M, Koyama T, Kim S, et al. 2018. Microscopic investigation into the electric field effect on proximity-induced magnetism in Pt. *Phys. Rev. Lett.* 120:157203
92. Fert A, Cros V, Sampaio J. 2013. Skyrmions on the track. *Nat. Nanotechnol.* 8:152–56
93. Thiaville A, Rohart S, Jué É, Cros V, Fert A. 2012. Dynamics of Dzyaloshinskii domain walls in ultrathin magnetic films. *Europhys. Lett.* 100:57002
94. Sampaio J, Cros V, Rohart S, Thiaville A, Fert A. 2013. Nucleation, stability and current-induced motion of isolated magnetic skyrmions in nanostructures. *Nat. Nanotechnol.* 8:839–44
95. Yang S-H, Ryu K-S, Parkin S. 2015. Domain-wall velocities of up to 750 ms^{-1} driven by exchange-coupling torque in synthetic antiferromagnets. *Nat. Nanotechnol.* 10:221–26
96. Srivastava T, Schott M, Juge R, Krizakova V, Belmeguenai M, et al. 2018. Large-voltage tuning of Dzyaloshinskii–Moriya interactions: a route toward dynamic control of skyrmion chirality. *Nano Lett.* 18:4871–77
97. Bhattacharya D, Razavi SA, Wu H, Dai B, Wang KL, Atulasimha J. 2020. Creation and annihilation of non-volatile fixed magnetic skyrmions using voltage control of magnetic anisotropy. *Nat. Electron.* 3:539–45
98. Yang Q, Cheng Y, Li Y, Zhou Z, Liang J, et al. 2020. Voltage control of skyrmion bubbles for topological flexible spintronic devices. *Adv. Electron. Mater.* 6:2000246
99. Zhang Y, Dubuis G, Doyle C, Butler T, Granville S. 2021. Nonvolatile and volatile skyrmion generation engineered by ionic liquid gating in ultrathin films. *Phys. Rev. Appl.* 16:014030
100. Qin P, Yan H, Fan B, Feng Z, Zhou X, et al. 2022. Chemical potential switching of the anomalous Hall effect in an ultrathin noncollinear antiferromagnetic metal. *Adv. Mater.* 34:2200487
101. Parkin S, More N, Roche K. 1990. Oscillations in exchange coupling and magnetoresistance in metallic superlattice structures: Co/Ru, Co/Cr, and Fe/Cr. *Phys. Rev. Lett.* 64:2304
102. Parkin SSP. 1991. Systematic variation of the strength and oscillation period of indirect magnetic exchange coupling through the 3*d*, 4*d*, and 5*d* transition metals. *Phys. Rev. Lett.* 67:3598
103. Duine R, Lee K-J, Parkin SS, Stiles MD. 2018. Synthetic antiferromagnetic spintronics. *Nat. Phys.* 14:217–19
104. Néel L. 1952. Antiferromagnetism and ferrimagnetism. *Proc. Phys. Soc. A* 65:869–85
105. Kim SK, Beach GS, Lee K-J, Ono T, Rasing T, Yang H. 2022. Ferrimagnetic spintronics. *Nat. Mater.* 21:24–34
106. Baltz V, Manchon A, Tsoi M, Moriyama T, Ono T, Tserkovnyak Y. 2018. Antiferromagnetic spintronics. *Rev. Mod. Phys.* 90:015005
107. Kim K-J, Kim SK, Hirata Y, Oh S-H, Tono T, et al. 2017. Fast domain wall motion in the vicinity of the angular momentum compensation temperature of ferrimagnets. *Nat. Mater.* 16:1187–92

108. Caretta L, Mann M, Büttner F, Ueda K, Pfau B, et al. 2018. Fast current-driven domain walls and small skyrmions in a compensated ferrimagnet. *Nat. Nanotechnol.* 13:1154–60
109. Bläsing R, Ma T, Yang S-H, Garg C, Dejene FK, et al. 2018. Exchange coupling torque in ferrimagnetic Co/Gd bilayer maximized near angular momentum compensation temperature. *Nat. Commun.* 9:4984
110. Cai K, Zhu Z, Lee JM, Mishra R, Ren L, et al. 2020. Ultrafast and energy-efficient spin–orbit torque switching in compensated ferrimagnets. *Nat. Electron.* 3:37–42
111. Wang Y, Li C, Zhou H, Wang J, Chai G, Jiang C. 2021. Unusual anomalous Hall effect in the ferrimagnetic GdFeCo alloy. *Appl. Phys. Lett.* 118:071902
112. Parkin SSP, Jiang X, Kaiser C, Panchula A, Roche K, Samant M. 2003. Magnetically engineered spintronic sensors and memory. *Proc. IEEE* 91:661–80
113. Nogués J, Sort J, Langlais V, Skumryev V, Suriñach S, et al. 2005. Exchange bias in nanostructures. *Phys. Rep.* 422:65–117
114. Zehner J, Huhnstock R, Oswald S, Wolff U, Soldatov I, et al. 2019. Nonvolatile electric control of exchange bias by a redox transformation of the ferromagnetic layer. *Adv. Electron. Mater.* 5:1900296
115. Jungwirth T, Marti X, Wadley P, Wunderlich J. 2016. Antiferromagnetic spintronics. *Nat. Nanotechnol.* 11:231–41
116. Chen X, Zhou X, Cheng R, Song C, Zhang J, et al. 2019. Electric field control of Néel spin–orbit torque in an antiferromagnet. *Nat. Mater.* 18:931–35
117. Chiang CC, Huang SY, Qu D, Wu PH, Chien CL. 2019. Absence of evidence of electrical switching of the antiferromagnetic Néel vector. *Phys. Rev. Lett.* 123:227203
118. Churikova A, Bono D, Neltner B, Wittmann A, Scipioni L, et al. 2020. Non-magnetic origin of spin Hall magnetoresistance-like signals in Pt films and epitaxial NiO/Pt bilayers. *Appl. Phys. Lett.* 116:022410
119. Nakatsuji S, Kiyohara N, Higo T. 2015. Large anomalous Hall effect in a non-collinear antiferromagnet at room temperature. *Nature* 527:212–15
120. Nayak AK, Fischer JE, Sun Y, Yan B, Karel J, et al. 2016. Large anomalous Hall effect driven by a nonvanishing Berry curvature in the noncolinear antiferromagnet Mn3Ge. *Sci. Adv.* 2:e1501870
121. Novoselov K, Mishchenko A, Carvalho A, Castro Neto AH. 2016. 2D materials and van der Waals heterostructures. *Science* 353:aac9439
122. Novoselov KS, Geim AK, Morozov SV, Jiang D, Zhang Y, et al. 2004. Electric field effect in atomically thin carbon films. *Science* 306:666–69
123. Xi X, Wang Z, Zhao W, Park J-H, Law KT, et al. 2016. Ising pairing in superconducting $NbSe_2$ atomic layers. *Nat. Phys.* 12:139–43
124. Lu J, Zheliuk O, Leermakers I, Yuan NF, Zeitler U, et al. 2015. Evidence for two-dimensional Ising superconductivity in gated MoS_2. *Science* 350:1353–57
125. Zhang K, Feng Y, Wang F, Yang Z, Wang J. 2017. Two dimensional hexagonal boron nitride (2D-hBN): synthesis, properties and applications. *J. Mater. Chem. C* 5:11992–2022
126. Wu C-L, Yuan H, Li Y, Gong Y, Hwang HY, Cui Y. 2018. Gate-induced metal–insulator transition in MoS_2 by solid superionic conductor LaF_3. *Nano Lett.* 18:2387–92
127. Deng Y, Yu Y, Song Y, Zhang J, Wang NZ, et al. 2018. Gate-tunable room-temperature ferromagnetism in two-dimensional Fe_3GeTe_2. *Nature* 563:94–99
128. Jiang S, Li L, Wang Z, Mak KF, Shan J. 2018. Controlling magnetism in 2D CrI_3 by electrostatic doping. *Nat. Nanotechnol.* 13:549–53
129. Shalnikov A. 1938. Superconducting thin films. *Nature* 142:74
130. Zhang T, Cheng P, Li W-J, Sun Y-J, Wang G, et al. 2010. Superconductivity in one-atomic-layer metal films grown on Si(111). *Nat. Phys.* 6:104–8
131. Lu J, Zheliuk O, Chen Q, Leermakers I, Hussey NE, et al. 2018. Full superconducting dome of strong Ising protection in gated monolayer WS_2. *PNAS* 115:3551–56
132. de la Barrera SC, Sinko MR, Gopalan DP, Sivadas N, Seyler KL, et al. 2018. Tuning Ising superconductivity with layer and spin–orbit coupling in two-dimensional transition-metal dichalcogenides. *Nat. Commun.* 9:1427
133. Shi W, Ye J, Zhang Y, Suzuki R, Yoshida M, et al. 2015. Superconductivity series in transition metal dichalcogenides by ionic gating. *Sci. Rep.* 5:12534

134. Yoshida M, Iizuka T, Saito Y, Onga M, Suzuki R, et al. 2016. Gate-optimized thermoelectric power factor in ultrathin WSe_2 single crystals. *Nano Lett.* 16:2061–65
135. Hitz E, Wan J, Patel A, Xu Y, Meshi L, et al. 2016. Electrochemical intercalation of lithium ions into $NbSe_2$ nanosheets. *ACS Appl. Mater. Inter.* 8:11390–95
136. Song Y, Liang X, Guo J, Deng J, Gao G, Chen X. 2019. Superconductivity in Li-intercalated $1T-SnSe_2$ driven by electric field gating. *Phys. Rev. Mater.* 3:054804
137. Ying T, Wang M, Wu X, Zhao Z, Zhang Z, et al. 2018. Discrete superconducting phases in FeSe-derived superconductors. *Phys. Rev. Lett.* 121:207003
138. Nakagawa Y, Kasahara Y, Nomoto T, Arita R, Nojima T, Iwasa Y. 2021. Gate-controlled BCS-BEC crossover in a two-dimensional superconductor. *Science* 372:190–95
139. Tang M, Huang J, Qin F, Zhai K, Ideue T, et al. 2022. Continuous manipulation of magnetic anisotropy in a van der Waals ferromagnet via electrical gating. *Nat. Electron.* 6:28–36
140. Nakagawa Y, Saito Y, Nojima T, Inumaru K, Yamanaka S, et al. 2018. Gate-controlled low carrier density superconductors: toward the two-dimensional BCS-BEC crossover. *Phys. Rev. B* 98:064512
141. Samarth N. 2017. Magnetism in flatland. *Nature* 546:216–17
142. Mermin ND, Wagner H. 1966. Absence of ferromagnetism or antiferromagnetism in one-or two-dimensional isotropic Heisenberg models. *Phys. Rev. Lett.* 17:1133
143. Huang B, Clark G, Navarro-Moratalla E, Klein DR, Cheng R, et al. 2017. Layer-dependent ferromagnetism in a van der Waals crystal down to the monolayer limit. *Nature* 546:270–73
144. Gong C, Li L, Li Z, Ji H, Stern A, et al. 2017. Discovery of intrinsic ferromagnetism in two-dimensional van der Waals crystals. *Nature* 546:265–69
145. Bedoya-Pinto A, Ji J-R, Pandeya A, Gargiani P, Valvidares M, et al. 2021. Intrinsic 2D-XY ferromagnetism in a van der Waals monolayer. *Science* 374:616–20
146. Gerstner W, Sprekeler H, Deco G. 2012. Theory and simulation in neuroscience. *Science* 338:60–65
147. Deng X, Wang SQ, Liu YX, Zhong N, He YH, et al. 2021. A flexible Mott synaptic transistor for nociceptor simulation and neuromorphic computing. *Adv. Electron. Mater.* 31:2101099
148. Li G, Xie D, Zhong H, Zhang Z, Fu X, et al. 2022. Photo-induced non-volatile VO_2 phase transition for neuromorphic ultraviolet sensors. *Nat. Commun.* 13:1729
149. Yang CS, Shang DS, Liu N, Fuller EJ, Agrawal S, et al. 2018. All-solid-state synaptic transistor with ultralow conductance for neuromorphic computing. *Adv. Electron. Mater.* 28:1804170
150. Sharbati MT, Du Y, Torres J, Ardolino ND, Yun M, Xiong F. 2018. Low-power, electrochemically tunable graphene synapses for neuromorphic computing. *Adv. Mater.* 30:1802353

Annual Review of Materials Research

Volume 53, 2023

Contents

Indexes

Errata

An online log of corrections to *Annual Review of Materials Research* articles may be found at http://www.annualreviews.org/errata/matsci